Hubs of long-distance co-alteration in brain pathology

FRANCO CAUDA[1,2*], LORENZO MANCUSO[1,2*], ANDREA NANI[1,2], JORDI MANUELLO[1,2], DONATO LILOIA[1,2], GABRIELE GELMINI[2], LINDA FICCO[2], ENRICO PREMI[3,4], SERGIO DUCA[1], TOMMASO COSTA[1,2]

[1]GCS-fMRI, Koelliker Hospital and Department of Psychology, University of Turin, Turin, Italy

[2]FOCUS Lab, Department of Psychology, University of Turin, Turin, Italy

[3]Stroke Unit, Azienda Socio Sanitaria Territoriale Spedali Civili, Spedali Civili Hospital, Brescia, Italy

[4]Centre for Neurodegenerative Disorders, Neurology Unit, Department of Clinical and Experimental Sciences, University of Brescia, Brescia, Italy

* *These authors contributed equally to this work*

Corresponding author:

Franco Cauda, PhD

FocusLab and GCS fMRI, Koelliker Hospital and Department of Psychology

University of Turin

e-mail: franco.cauda@unito.it

Abstract

The exact mechanisms at the root of pathologic anatomical covariances are still unknown. It is nonetheless becoming clearer that the impact of brain diseases is more convincingly represented in terms of *co*-alterations rather than in terms of localization of alterations. According to this view, neurological and psychiatric conditions might be seen as whole-brain patterns of modifications. In this context, the physical distance between two co-altered areas may provide insightful information about how pathology develops across the brain, assuming that long-range co-alterations might be relevant features of pathological networks. To demonstrate this hypothesis, we calculated the probability of co-alteration between brain areas across a large database of voxel-based morphometry studies of psychiatric and neurological disorders, and we investigated the physical (Euclidean) distance of the edges of the resulting network. Such analysis produced a series of observations relevant for the understanding of pathology, which range from unanticipated results to the recognition of regions of well-known functional and clinical relevance. For instance, it emphasizes the importance of the anterior and dorsal prefrontal cortices in the distribution of the disease-related alterations, as well as a specular asymmetry of gray matter decreases and increases between the hemispheres. Also, the analyses of schizophrenia and Alzheimer's disease show that long-distance co-alterations are able to identify areas involved in pathology and symptomatology. Moreover, the good concordance between the measure of the mean physical distance and that of functional degree centrality suggests that co-alterations and connectivity are intimately related. These findings highlight the importance of analyzing the physical distance in pathology, as the areas characterized by a long mean distance may be considered as hubs with a crucial role in the systems of alterations induced by brain diseases.

Keywords: physical distance, VBM, network degeneration, pathology spread, schizophrenia, Alzheimer's disease

Introduction

Converging evidence is revealing that the impact of diseases on brain structure is better appreciated not as the simple spatial distribution of lesions but as a system of interrelated alterations affecting networks (Evans, 2013). This makes sense in neurodegenerative diseases, where misfolded proteins frequently spread from one area to another in a prion-like fashion (Guest *et al.*, 2011; Goedert *et al.*, 2017). This mechanism has been put forward to explain the development of anatomical alterations observed in such diseases in terms of connectivity pathways, along which pathological proteins (proteinopathy) or other toxic agents can propagate (Seeley *et al.*, 2009; Saxena and Caroni, 2011; Warren *et al.*, 2012, 2013; Mandelli *et al.*, 2016; Manuello *et al.*, 2018). However, the network-like account of co-alterations seems to provide insights also in clinical conditions that do not have a neurodegenerative origin, such as schizophrenia, autism, obsessive-compulsive disorder, depression, and chronic pain (Cauda *et al.*, 2014, 2017, 2018*a*; Wheeler *et al.*, 2015, 2017; Tatu *et al.*, 2018). Furthermore, transdiagnostic meta-analyses merging data of studies about psychiatric and neurologic diseases support the following ideas: i) the most affected areas of the brain correspond to the hubs of the functional and structural connectomes (Crossley *et al.*, 2014), and ii) the distribution and development of co-alterations are mainly explained by functional and structural connectivity constraints (Cauda *et al.*, 2018*b*). Therefore, the anatomical substrate of brain disorders might be better accounted for by patters of *co-alterations* than by the simple localization of a series of unrelated alterations.

A relevant feature of brain organization is the physical distance between interconnected areas. The small-world networks of the human connectome are composed by several clusters of short-range connectivity, linked together by long-range connections (Watts *et al.*, 1998; Sporns and Zwi, 2004; Achard *et al.*, 2006). Within an evolutionary perspective, the brain evolved to match a trade-off between minimizing wiring cost and allowing a fast, efficient and resilient information flow (Laughlin and Sejnowski, 2003; Bullmore and Sporns, 2012). Nodes of long-range connectivity are to be considered central hubs of the connectome, as they tend to be connected with many other nodes, which makes them crucial in the interplay between segregation and integration that shapes brain structure

and function (Bullmore and Sporns, 2012; Alexander-Bloch *et al.*, 2013; Liao *et al.*, 2013). This organization is likely to be associated with the distribution patterns of neuropathological alterations, as brain hubs with high centrality are also the regions more likely to be affected by pathology (Crossley *et al.*, 2014). Interestingly, both functional (Alexander-Bloch *et al.*, 2013) and anatomical covariance (Bassett *et al.*, 2008) networks (Bassett *et al.*, 2008) of diseases such as schizophrenia, have been associated with altered values of physical distance. Higher-order associative brain regions, which are more prone to be targeted by diseases (Crossley *et al.*, 2014), are characterized by a long physical distance and a high centrality (Sepulcre *et al.*, 2010). So, if connectivity influences the development of pathology (He *et al.*, 2007; Seeley *et al.*, 2009; Zhou *et al.*, 2012; Mandelli *et al.*, 2016, Cauda *et al.*, 2018*b*), the spatial distribution of the physical distance of co-alterations might provide an insightful indication of how pathology is distributed across the brain. It would be also interesting to compare such information with a measure of centrality from a normative connectome, so as to test if there is a correlation between abnormal distance and connectivity. This would help clarify the relationship between co-alteration and connectivity, as well as understand better the complex systems of alterations in action on the brain.

In the present study we assessed the mean physical distance of co-alterations and its relationship with functional degree centrality (DC) in a meta-analytic, transdiagnostic way, so as to identify the cerebral areas that are more involved in long-range systems of pathological modifications. We obtained from the BrainMap database both voxel-based morphometry (VBM) and activation data to be used in a meta-analytic technique based on the Patel's κ (Patel *et al.*, 2006, Cauda *et al.*, 2018*a*; Mancuso *et al.*, 2019). This transdiagnostic approach was motivated by the assumption that the mechanisms underlying the phenomenon of co-alteration seem to be related to normative brain connectivity (Buckholtz and Meyer-Lindenberg, 2012, Cauda *et al.*, 2018*b*). We therefore constructed networks of pathologic co-alterations of gray matter (GM) decreases or increases and calculated the mean physical (Euclidean) distance for each brain region. Then we compared the map of physical distance with a map of meta-analytic degree

centrality of co-activations, so as to see whether or not the most connected areas of the functional healthy brain are also those with the longest co-alterations. Moreover, we investigated the transdiagnostic variability of each voxel and network, which allowed to assess the convergence of the most important pathologies in respect to their distance of co-alteration. Finally, taking schizophrenia and Alzheimer's disease as representative examples of a single-pathology approach for psychiatric and neurologic diseases, we observed their maps of mean physical distance of co-alterations. This investigation showed that the anatomical distribution of the mean physical distance can provide an insightful index of the pathologic spread of single diseases.

Materials and methods

Collection of data

In the present study the Cochrane Collaboration definition of meta-analysis (Green *et al.*, 2008) was adopted and the selection of articles was conducted referring to the "PRISMA statement" international guidelines (Liberati *et al.*, 2009; Moher *et al.*, 2009). Neuroimaging experiments eligible for the analysis were retrieved from BrainMap (http://brainmap.org/) (Fox and Lancaster, 2002; Fox *et al.*, 2005; Laird *et al.*, 2005; Vanasse *et al.*, 2018). BrainMap is an open access online database constituted by over 15000 neuroimaging experiments and 120000 locations in stereotaxic brain space. The database has two sections for VBM and functional data sets.

The VBM BrainMap section was queried (November 2017) with the following algorithms:

1) [Experiments Context is Disease] AND [Experiment Contrast is Gray Matter] AND [Experiments Observed Changes is Controls>Patients];

2) [Experiments Context is Disease] AND [Experiment Contrast is Gray Matter] AND [Experiments Observed Changes is Patients>Controls].

The first step consisted in the codification of the VBM data set following the ICD-10 classification (World Health Organisation, 1992). Subsequently, full-text articles were analyzed in order to verify that they conformed with the following criteria: a) being an original work published in a peer-reviewed English language journal; b) performing a whole brain VBM analysis technique; c) including a matched comparison between a pathological group and a group of healthy subjects; d) reporting GM decrease/increase changes in the pathological sample; e) adopting a specified VBM analysis; f) referring to a specific stereotaxic space (e.g. Montreal Neurological Institute space or Talairach/Tournoux atlas) as regards GM increase/decrease changes. On the basis of these criteria we deemed eligible 912 experiments for GM decreases and 350 for GM increases. Descriptive information of interest was extracted from each full-text article fulfilling the abovementioned criteria. As a further specification, all the experiments not coded with F (i.e. mental, behavioral and neurodevelopmental disorders) or G (i.e. diseases of the nervous system) labels were excluded from the analysis. Moreover, studies related to codes that could not be considered as primary brain disorders (i.e. F10: Alcohol related disorders; F15: Other stimulant related disorders; F28: Other psychotic disorder not due to a substance or known physiological condition; F91: Conduct disorders; G11: Hereditary ataxia; G43: Migraine; G44: Other headache syndromes; G47: Sleep disorders; G50: Disorders of trigeminal nerve; and G71: Primary disorders of muscles) were also excluded. Articles including less than 8 subjects were excluded as well. This lower bound was chosen in accordance with the work of Scarpazza and colleagues (Scarpazza *et al.*, 2015), whose work demonstrated that VBM experiments based on an equivalent sample should not be biased by an increased false positive rate. At the end of the selection procedure, 642 remaining experiments for the GM decreases (for 15820 subjects and 7704 foci) and 204 remaining experiments for the GM increases (for 4966 subjects and 2244 foci) were included in the analyses. We also calculated two single-disease co-alteration networks using only on the data of schizophrenia and Alzheimer's disease (see Supplementary Fig. 1 and Supplementary Table 3 and 4).

Finally, a systematic search was conducted through the entire functional data set of BrainMap with the following query:

> [Experiments Context is Normal Mapping] AND [Experiments Activation is Activations Only] AND [Subjects Diagnosis is Normals].

This search produced 2376 articles, for a total of 13148 experiments, 112 paradigm classes and 68152 subjects (see Supplementary Fig. 1 and Supplementary Table 6). Finally, we converted all locations reported in MNI into Talairach space using the Lancaster's icbm2tal transform (Lancaster *et al.*, 2007).

Modeled alteration maps

To obtain the alteration maps from the BrainMap foci, we adopted the anatomical likelihood estimation (ALE) framework (Eickhoff *et al.*, 2009, 2012; Turkeltaub *et al.*, 2012) to produce a modeled alteration (MA) map for each experiment. To build the MA maps, every focus of each experiment is taken as the central point of a 3-dimensional Gaussian distribution of probability:

$$p(d)=\frac{1}{\sigma^3\sqrt{(2\pi)^3}}e^{\frac{d^2}{2\sigma^2}}$$

In this formula d represents the Euclidean distance between the voxels and each considered focus, while e indicates the spatial uncertainty. The standard deviation is obtained through the full-width half-maximum (FWHM), which is defined as follows:

$$\sigma=\frac{FWHM}{\sqrt{8\ln 2}}$$

Co-alteration matrix calculation

The brain was partitioned on the basis of an anatomical atlas derived from the Talairach Daemon atlas with a resolution of 2 mm (Lancaster *et al.*, 2000); a co-alteration matrix resulted from all the possible couples of brain areas. In the resulting ExN matrix, each of E row stands for an experiment, while each of N column reports a node; in the present study the matrix included 642 experiments (VBM contrasts) x 1105 nodes for the decrease condition, and 204 experiments x 1105 nodes for the increase condition. For each experiment, a given brain region was considered to be altered if the experiment MA map showed 20% or more of significant voxels within the region. The choice of this threshold is arbitrary, but it has already been proven that it do not affect the results significantly (Mancuso *et al.*, 2019). The use of Patel's κ index allowed us to obtain the co-alteration strength between the nodes (Patel *et al.*, 2006); then, a probability distribution of joint alteration occurrences for every couple of nodes was created following a Bernoulli model of data generation. In other words, given two nodes (*a* and *b*), we can determine all their conjoint states of alteration as follows: i) *a* and *b* are both altered; ii) *a* is altered and *b* is not; iii) *b* is altered and *a* is not; iv) neither *a* nor *b* are altered. Thus, frequencies of these four cases recurring in all the experiments could be described by the following probability formulas:

$$\vartheta_1 = P(a=1, b=1)$$

$$\vartheta_2 = P(a=1, b=0)$$

$$\vartheta_3 = P(a=0, b=1)$$

$$\vartheta_4 = P(a=0, b=0)$$

		node a		
		Altered	Unaltered	
node b	Altered	ϑ_1	ϑ_3	$\vartheta_1+\vartheta_3$
	Unaltered	ϑ_2	ϑ_4	$\vartheta_2+\vartheta_4$
		$\vartheta_1+\vartheta_2$	$\vartheta_3+\vartheta_4$	1

Table 1: Marginal probabilities between altered and unaltered regions.

These probabilities stand for the conjoint state frequencies of a couple of nodes (a and b) in the four possible combinations. Table 1 contains the marginal probabilities. Obtaining these probabilities allowed us to use the Patel's κ index to create the correlation matrix including each couple of brain areas. Patel's κ informs about the likelihood that two nodes (a and b) are co-altered, namely, it expresses the probability that a and b are altered independently of each other. Patel's κ is defined as follows:

$$\kappa = \frac{(\vartheta_1 - E)}{D(max(\vartheta_1) - E) + (1 - D)}$$

where

$$E = (\vartheta_1 + \vartheta_2)(\vartheta_1 + \vartheta_3)$$

$$D = \begin{cases} \dfrac{\vartheta_1 - E}{2(max(\vartheta_1) - E)} + 0.5, if\ \vartheta_1 \geq E \\ 0.5 - \dfrac{\vartheta_1 - E}{2(E - min(\vartheta_1))}, otherwise \end{cases}$$

$$max(\vartheta_1) = min\ (\vartheta_1 + \vartheta_2, \vartheta_1 + \vartheta_3)$$

$$min(\vartheta_1) = max\ (0, 2\vartheta_1 + \vartheta_2 + \vartheta_3 - 1)$$

The numerator of the fraction is the difference between the likelihood that a and b are altered together and their expected joint alteration in a condition of independence, and the denominator is a weighted normalizing constant. $Min(\vartheta_1)$ represents the maximum value of conjoint probability $p(a,b)$, given $p(a)$ and $p(b)$, whereas $max(\vartheta_1)$ represents the minimum value of $p(a,b)$, given $p(a)$ and $p(b)$. Patel's κ index returns values ranging from –1 and 1. A value of $|\kappa|$ that is close to 1 characterizes a high co-alteration. The statistical significance of Patel's κ is assessed by means of a simulation of a generative model of data

based on the Monte Carlo's algorithm. Specifically, the algorithm computes an estimate of $p(\kappa|z)$ by sampling a Dirichlet distribution and determining the proportion of the samples in which $\kappa > e$, where e is the threshold of statistical significance. The resulting co-alteration matrix returns values that are proportional to the statistical relationship between the patterns of brain areas' alterations taken into account.

Functional connectivity matrix

The meta-analytic connectivity was obtained applying the same method for the construction of the co-alteration matrix (i.e. Patel's κ index calculated on each couple of brain areas) to the BrainMap functional database of activations of healthy subjects.

Measurement of the mean distance and calculation of the meta-analytic degree centrality

For each significant statistical association between two regions a and b in the co-alteration (or co-activation) matrix, we calculated the respective physical distance as the Euclidean distance between the centroids of a and b in the Talairach Daemon atlas. Then, for each node, the distance of its connections was averaged to obtain its mean physical distance, and such value was assigned to the whole region to obtain a map.

To calculate the degree centrality (DC) of co-activation on the functional data we employed the Brain Connectivity Toolbox algorithms (Rubinov and Sporns, 2010). Specifically, DC was defined as the number of edges incident to a node.

Comparison between maps

In order to evaluate the similarity between the distance of the co-alteration map and the functional DC map, the correlation between these maps was calculated. To establish the involvement of each brain area to the correlation between the two maps we applied the voxels' contribution to correlation (VCC) technique (Mancuso *et al.*, 2019). This *leave-one-out* procedure recursively computes the correlation between each couple of maps, subtracting a voxel at every run (the same voxel for both the maps). To create a map

showing the contribution of each voxel to the correlation, the difference between the correlation value calculated in the whole maps and the correlation value obtained after the exclusion of each couple of voxels is associated to the singular voxel. Therefore, it is possible to visualize the extent to which the correlation value decreases or increases depending on the subtraction of each couple of corresponding voxels from the calculation. The normalized version of this map (transformed in order to range from –1 to 1) represents the stability of correlation and describes the contribution of each voxel to the correlation. This procedure allows to characterize voxels as positive or negative. The former contribute positively to the correlation, as their removal decreases the correlation value; the latter contribute negatively to the correlation, as their removal increases the correlation value.

Leave-one-pathology-out

The leave-one-pathology-out is a validation technique used to evaluate both the variability and generalizability of measurements. The procedure for the calculation of the mean physical distance described above was performed several times, each run excluding a different pathology. For all the outcomes resulting from each measurement the voxel-wise standard deviation was calculated to verify the degree of variability and consistency of the different measurements with regard to each pathology.

Results

Maps of the mean physical distance

The map of the mean physical distance of co-alterations related to GM decreases show higher peaks in the dorsal and anterior regions of the left prefrontal cortex (PFC), and the bilateral medial temporal lobe (MTL). Left posterior insula, left postcentral gyrus, right precentral gyrus and clusters in the bilateral temporal and occipital lobes are also involved. The map of GM increases is characterized by more extreme values compared to that of GM decreases, thus, despite the low magnitude of many voxels, certain areas reach higher values than those observed in the other map. Those areas are the bilateral pre- and

postcentral gyri, the right anterior PFC, an inferior cluster in the bilateral occipital cortex, and the left medial cuneus (Fig. 1).

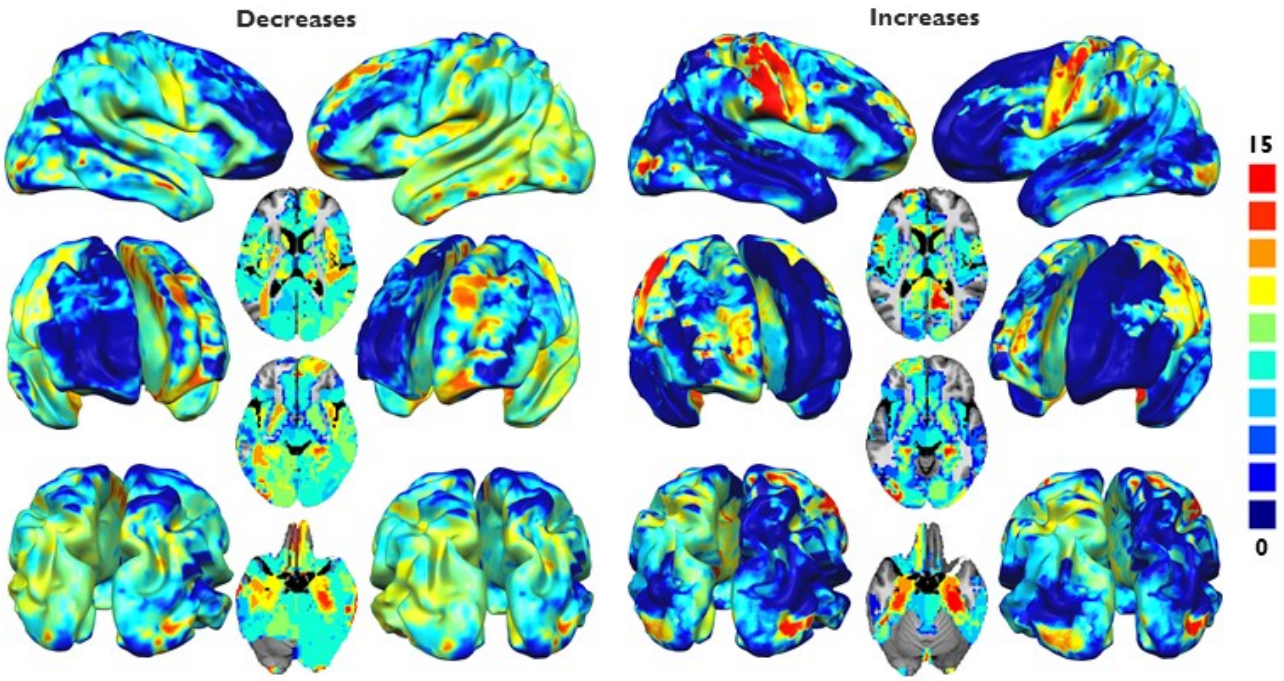

Figure 1. Parametric mapping of the mean distance of co-alterations, divided for decreases and increases. Higher values indicate increasing mean distance.

The sensorimotor network, the default mode network (DMN), the salience network (SN), the dorsal attention network (DAN), and the thalamus and basal ganglia are the systems where both GM increases and GM decreases show long distance co-alterations. GM decreases show longer distance co-alterations than the GM increases in the auditory network and the cerebellum (Fig. 2).

Comparison with the map of functional degree centrality

The functional meta-analytic DC map reveals the presence of normative hubs in the bilateral superior temporal cortex, bilateral occipital cortex, right temporoparietal junction and right inferior prefrontal gyrus. The systems that present the longer distance co-alterations are the sensorimotor network, the SN and the auditory network. The correlations between the functional DC map and the maps of GM decreases and increases are $r=0.73$ and $r=0.57$, respectively. The VCC analysis reports a high concordance between the functional degree map and both the GM increases and decreases mean distance co-alteration maps in most of the voxels, except for those belonging to the right

PFC and the left middle frontal gyrus (MFG) in the GM decreases map, and those belonging to the left PFC, right MFG, and bilateral temporal cortices in the GM increases map (Fig. 2).

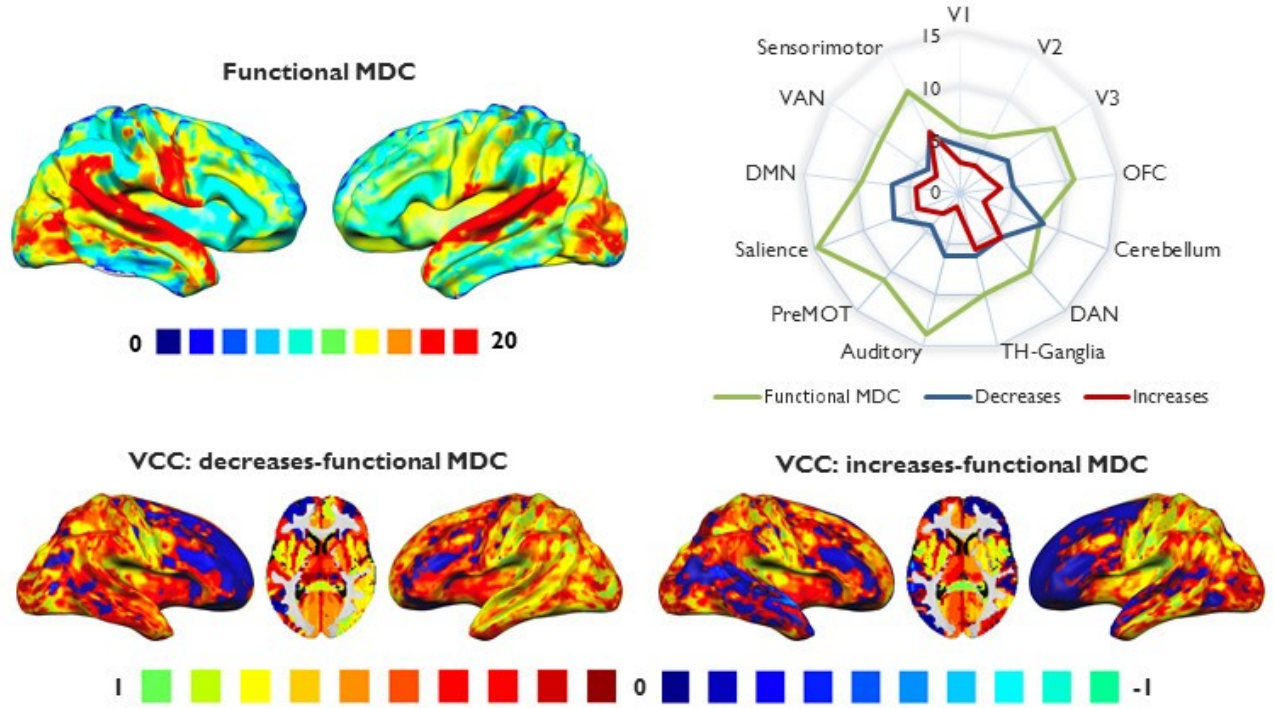

Figure 2. Comparison between maps of mean distance and the functional degree centrality. Top left panel: surface mapping of the functional meta-analytic degree centrality (functional MDC) obtained with co-activations. Higher values indicate higher degree centrality. Top right panel: radar chart comparing the average values of mean distance of decreases, increases and of functional meta-analytic degree centrality for each of the following networks: visual networks 1, 2 and 3 (V1, V2 and V3), orbitofrontal cortex (OFC), cerebellum, dorsal attentional network (DAN), thalamus and basal ganglia, auditory network, premotor network, salience network, default mode network (DMN), ventral attentional network (VAN), and sensorimotor network. Bottom panel: parametric mapping of the voxels' contribution to correlation analysis between the functional meta-analytic degree centrality map and the mean distance co-alteration maps of decreases and increases. Positive values indicate areas of concordance between the maps, negative values indicate discordance.

Leave-one-pathology-out analysis

The regions with the highest variability across diseases are the bilateral (but especially right) inferior frontal gyrus (IFG), the bilateral insula, the bilateral temporal lobe and the bilateral occipital lobe for the map of GM decreases; the right pre- and postcentral gyri, the left MFG, the left angular gyrus and the right occipital lobe for the map of the GM increases (Fig. 3). The two maps involve different systems, especially the sensorimotor

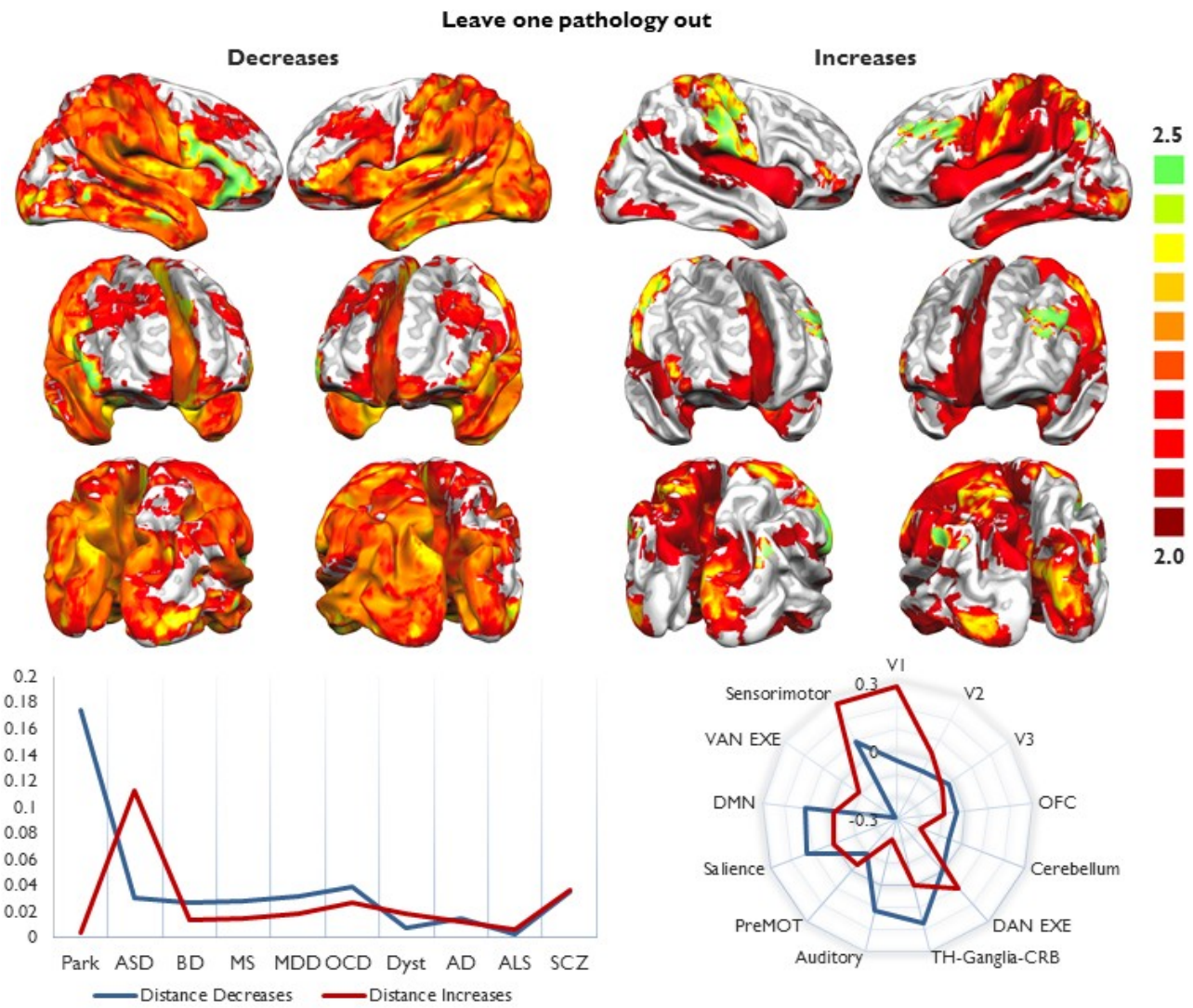

Figure 3. Top panel: surface mapping of the transdiagnostic variance of the mean distance maps of decreases and increases. Higher values indicate higher variance, that is, the voxels whose value in the mean distance map is more variable across pathologies. Bottom left panel: spatial variability of the changes introduced removing each pathology from the database. Higher values represent the pathologies whose changes were more uneven across resting state networks. Bottom right panel: values of variance of the mean distance of decreases and increases divided by resting state networks: isual networks 1, 2 and 3 (V1, V2 and V3), orbitofrontal cortex (OFC), cerebellum, dorsal attentional network (DAN), thalamus and basal ganglia, auditory network, premotor network, salience network, default mode network (DMN), ventral attentional network (VAN), and sensorimotor network.

network, the DMN, the SN, the auditory network and the thalamus and basal ganglia for the GM decreases, and the sensorimotor network and V1 for the GM increases (Fig. 3).

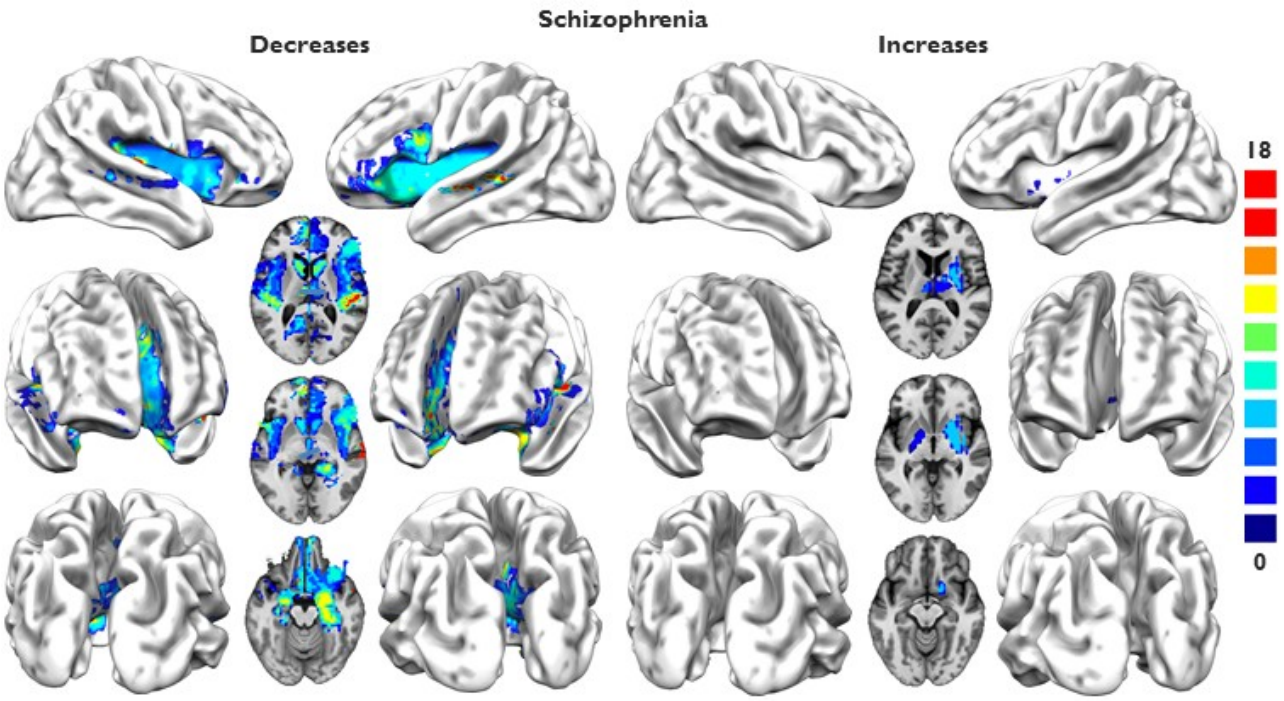

Figure 4. Parametric mapping of the mean distance of co-alterations in schizophrenia, divided for decreases and increases. Higher values indicate increasing mean distance.

Extracting a pathology from our database produced changes that could be unevenly distributed between the networks. For instance, the removal of Parkinson's disease from the GM decrease dataset produced changes with the widest spatial variability, but when studies about this pathology were removed from the GM increase database the produced changes were mostly homogeneous. On the contrary, amyotrophic lateral sclerosis, Alzheimer's disease and schizophrenia were the disorders whose removal produced the most similar impact regarding the spatial variance of changes on both the maps of GM increases and decreases (Fig. 3). These differences cannot be explained solely by the number of experiments of each pathology in the database, as disorders well represented as schizophrenia and Alzheimer's disease had a minor impact on the results when removed compared to other less represented disorders (see Supplementary Tables 1, 2 and 5).

Although analytic comparisons between disorders cannot be made, because of the uneven distribution of experiments, these findings can be considered as an indication of how different pathologies are characterized by various patterns of co-alteration distances.

Schizophrenia and Alzheimer's disease

With regard to the map of GM decreases of schizophrenia (Fig. 4), the left auditory cortex shows the longest mean distance co-alterations (and, albeit less strongly, the right auditory cortex is also involved). Small clusters can be found in the right superior temporal sulcus (STS). The bilateral insula is widely involved, as well as the left IFG (especially in its posterior portion), the bilateral anterior cingulate cortex (ACC), the MTL (especially the left one), and the bilateral caudate. The map of GM increases shows long distance co-alterations mainly in the left putamen.

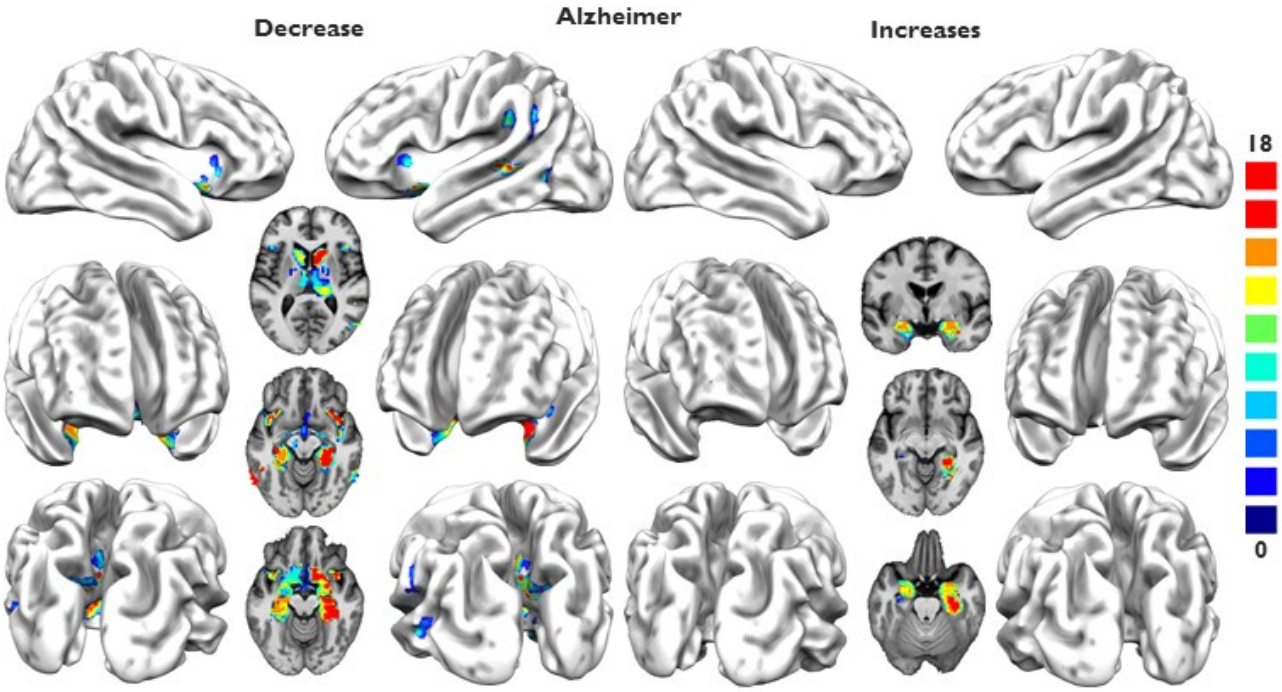

Figure 5. Parametric mapping of the mean distance of co-alterations in Alzheimer's disease, divided for decreases and increases. Higher values indicate increasing mean distance.

With regard to the map of GM decreases of Alzheimer's disease (Fig. 5), long distance co-alterations characterize the caudate (especially the left one), the MTL (especially the left one), the bilateral IFG pars orbitalis, the left orbital cortex, certain clusters in the bilateral anterior insula, and a cluster in the STS. In turn, the map of GM increases shows long distance co-alterations just in the bilateral MTL (especially the left one).

Discussion

This study investigates, for the first time, the spatial distribution of the physical distance of co-alterations, highlighting that this type of measurement is able to provide insightful indications about the distribution patterns of GM alterations related to brain diseases. Findings show a spatial distribution of the mean physical distance of transdiagnostic co-alterations that can vary between areas in interesting and meaningful ways. For instance, GM decreases exhibit longer distance co-alterations in the left hemisphere compared to the right one (Fig. 1). Intriguingly, this suggests an asymmetry in the pathological involvement of the left and right hemispheres, as the former appears to show more global patterns of co-alterations, while the latter appears to be characterized by more local covariances. The left dorsal and anterior PFC tend to co-alter with distant areas. In addition, the lateral parts of PFC show low transdiagnostic variance (Fig. 3), which means that they present long-range co-alterations related to GM decreases in a wide range of pathologies. This is consistent with the low mean distance variability exhibited by the DAN (Fig. 3), as well as with the clinical observation of executive functions deficits in many diseases (Goodkind *et al.*, 2015; McTeague *et al.*, 2016). On the contrary, the left medial anterior PFC, and especially a part of left medial dorsal PFC, display high variance, thus suggesting that the medial PFC may be involved in long-range co-alterations in several disorders.

The MTL shows long-range co-alterations related to GM decreases. Given its involvement in memory and learning, it is likely for it to be co-altered with many other associative areas in a variety of diseases, causing symptoms of memory loss, for instance in neurodegenerative conditions such as Alzheimer's disease, or symptoms of inappropriate memory and limbic responses that are frequently observed in the ruminations characterizing depression (Sheline *et al.*, 2009). Significantly, the MTL is part of the DMN (Buckner *et al.*, 2008; Andrews-Hanna *et al.*, 2010), which is one of the most involved brain networks in long-range GM decreases (Fig. 3).

It is interesting to observe that the map of the mean physical distance of co-alterations related to the GM increases shows higher values in the right hemisphere than in the left, in spite of the left prevalence of the map related to the GM decreases. This difference is

particularly noted in the dorsal and anterior lateral PFC, which is a region of significant longer co-alterations in the left hemisphere of the GM decreases' map, while in the GM increases' map this region presents longer co-alterations in the right hemisphere (Fig. 1). Such an asymmetry between the maps of GM increases and of GM decreases might be due to an effect of compensation (Cauda *et al.*, 2014). In other words, while the left PFC is pathologically involved in a network of long-distance co-alterations of GM decreases the right PFC could compensate the disruption of its left homologue by being involved in a network of long-range increases. However, it cannot be excluded that both GM increases and GM decreases are primary effects of the disease itself. Future studies are needed in order to corroborate these findings and to explain the mechanism underlying this interesting asymmetry.

Other areas of long-distance co-alterations related to the map of GM increases are the pre- and postcentral gyri, particularly within the right hemisphere. Indeed, the sensorimotor network is one of the most involved systems in the map of GM increases (Fig. 3). However, these regions are also characterized by high transdiagnostic variance (Fig. 2). Overall, the sensorimotor network exhibits long-distance co-alterations related to the map of GM increases, but its involvement is not consistent across diseases; in turn, the anterior and dorsal lateral PFC are characterized by a greater transdiagnostically involvement in both the maps of GM decreases (in the right hemisphere) and of GM increases (in the left hemisphere).

The map of physical distance of co-alterations resembles that of functional degree centrality

The investigation of the relationship between centrality and distance) provides evidence of a good convergence between the map of co-activation DC and those of physical distance of co-alteration, especially with the one related to the GM decreases. This strongly suggests that brain functional hubs are also the regions whose mean distance of co-alteration is longer. Save for the PFC, most of the cortical areas contribute positively to the correlation between functional DC and co-alteration distance. It should be observed that the frontal

voxels in the dorsal and anterior PFC displaying low convergence are not characterized by long transdiagnostic distance. On the contrary, the dorsal and anterior PFC show high convergence between co-activation centrality and co-alteration distance in the left hemisphere for the GM decreases, as well as in the right hemisphere for the GM increases, where long-distance co-alterations are found. In general, regions of long-distance co-alteration, such as the pre- and postcentral gyri and the insula, exhibit high consistency with the map of functional centrality (Fig. 2). Of note, pre- and postcentral gyri are found to be hubs of long-distance connectivity when short-rage connections are subtracted from the connectome (Esfahlani *et al.*, 2019).

One of the fundamental issues in the study of co-alterations is to understand the mechanism that is responsible for morphological co-variations of specific sets of areas in relation to a pathological process. Our analyses provide evidence of an interesting association between the distance of co-alterations and the functional DC. As brain hubs are supposed to be preferentially targeted by pathological alterations (Buckner *et al.*, 2009; de Haan *et al.*, 2012; Crossley *et al.*, 2014), the finding of a convergence between functional DC distribution and long-distance co-alteration areas suggests that brain regions which are more likely to be affected by diseases are also more likely to be co-altered with distant areas. A possible explanation might be that such regions are more susceptible to metabolic stress in virtue of their numerous connections and intense work of integration of different information (Crossley *et al.*, 2014). Although capable of explaining the high rate of damage undergone by hubs, this model alone fails to explain our findings: it would be unclear why areas of high metabolic stress should be co-altered with other distant regions. Conversely, the transneuronal spread hypothesis (Zhou *et al.*, 2012), which accounts for the pathologic progression with the diffusion of toxic agents such as misfolded proteins, seems to be more up to the task.

The idea that misfolded proteins are responsible for the pathological spread has found several supporting evidence in studies about neurodegenerative diseases (Seeley *et al.*, 2009; Guest *et al.*, 2011; Raj *et al.*, 2012; Warren *et al.*, 2012, 2013; Zhou *et al.*, 2012; Iturria-Medina *et al.*, 2014; Ahmed *et al.*, 2016; Goedert *et al.*, 2017), but has also been putatively

extended to psychiatric conditions. In fact, insoluble aggregates of disrupted-in-schizophrenia 1 (DISC1) were associated to sporadic cases of schizophrenia, bipolar disorder and depression (Leliveld *et al.*, 2008; Korth, 2012). In addition, *in vitro* studies have demonstrated that aggregates of DISC1 are able to transfer between cells via tunnelling nanotubes (Zhu *et al.*, 2017). These aggregates can selectively affect dopaminergic brain functioning at pre-synaptic and post-synaptic level (Dahoun *et al.*, 2017; Tropea *et al.*, 2018), and, as they are related to oxidative stress (Trossbach *et al.*, 2016), the transneuronal spread hypothesis is not incompatible with the metabolic stress model. On the contrary, both pathological mechanisms might be necessary for a hub to be damaged (Saxena and Caroni, 2011). According to this view, brain hubs are more vulnerable to deterioration, and in turn they can spread the alterations to the connected areas. Furthermore, given their high degree of connectivity and their role of integration of different clusters, hubs are generally linked to many distant regions, and this makes them ideal for spreading pathological alterations along several long-range connections.

It has also been suggested that alterations could propagate by means of a trophic factor release failure (Fornito *et al.*, 2015). In other words, the areas connected to the damaged region might suffer morphological GM decreases because they cease to receive trophic factors from them (Chao, 2003), or might reduce activity because of the lack of inputs, which could disrupt their activity-dependent trophic factors synthesis and release (Gall and Isackson, 1989; Blöchl and Thoenen, 1995; Kohara *et al.*, 2001), thus leading to a cascade of anatomical decreases. A disruption of the balance of the trophic mechanism, in form of an enhanced trophic release or a lack of growth-inhibitory signals (Perlson *et al.*, 2010), may also account for the generations of networks of GM increases. Of course, the effect of morphometric increase might be of iatrogenic nature (Navari and Dazzan, 2009; Hafeman *et al.*, 2012); however, this general explanation is not able to take into account the similarity between hubs of long-distance increase to that of FC. Thus, we suggest that a mixture of metabolic stress, toxic spread, trophic factor release disruption and shared vulnerability to genetic and environmental factors influence the distribution of both decrease and increase co-alteration along connectivity pathways (Cauda *et al.*, 2019).

Therefore, brain hubs might be not only extremely vulnerable to disorders but also substantially responsible for the long-range spread of morphological changes.

Analyses of schizophrenia and Alzheimer's disease

With regard to schizophrenia (Fig. 4), areas with long-distance co-alterations of GM decreases have auditory and linguistic roles; a finding that is in accordance with the auditory hallucinations affecting a portion of these patients (Neckelmann *et al.*, 2006; Plaze *et al.*, 2006; García-Martí *et al.*, 2008; Modinos *et al.*, 2009). Also the caudate and the MTL exhibit long-distance co-alterations, as well as the SN, which is in line with the involvement of this network in the disease (Kapur, 2003; White *et al.*, 2010; Palaniyappan and Liddle, 2012; Palaniyappan *et al.*, 2013; Manoliu *et al.*, 2014; Uddin, 2015; Liddle *et al.*, 2016, Cauda *et al.*, 2018*a*). Long co-alterations of GM increases are found especially in the left putamen, which is coherent with a study that found an increased putamen characterized by leftward asymmetry in schizophrenic patients (Okada *et al.*, 2016).

With regard to Alzheimer's disease (Fig. 5), long-distance co-alterations of GM increases and GM decreases are found especially in the left hippocampal formation, which is consistent with the assumption that the hippocampus may be the pathological epicentre, as well as with the observation that the left hemisphere is more affected than the right one (Loewenstein *et al.*, 1989; Braak *et al.*, 1993; Janke *et al.*, 2001; Thompson *et al.*, 2001, 2003, 2007; Buckner, 2005; Pievani *et al.*, 2011; Manuello *et al.*, 2018). Other regions with long-distance co-alterations of GM decreases are the caudate and the insula, with a major involvement in the left hemisphere. The finding that the left MTL is involved in long-distance co-alterations both of GM increases and of GM decreases in intriguing, and might be putatively explained by the effect of compensation, as if this region could be engaged in a system of increases that try to counteract to the damages induced by the disease. Although small posteromedial cortical clusters can be appreciated in the map of GM decreases (Fig. 5), the absence of large significant neocortical clusters might be due to the modest sensitivity of VBM to changes in the cortical ribbon compared to those in the hippocampal region (Diaz-De-Grenu *et al.*, 2014). As we have seen, the measurement of the

mean physical distance of co-alterations can identify clinically relevant areas, as they are associated with typical symptoms of brain disorders, and even the epicenters of pathological diffusion. In this regard, it should be emphasized that our analysis is considerably different from other volumetric studies: our methodology does not evaluate the size and number of alterations, but only if an alteration is associated with nearby or distant modifications. The two measures, therefore, do not necessarily converge, and the fact that our findings are in line with those provided by the scientific literature is a strong indication that the mean physical distance of co-alterations is an insightful instrument for detecting pathological features of diseases.

Limitations

A possible limitation of our analyses is that nodes were defined on the basis of an anatomical atlas; therefore, they may fail to account for more fine-grained distinctions in heterogeneous regions. This choice aimed to achieve a higher statistical power, as a voxel-wise technique may leave some voxels uncovered by a sufficient number of samples. It could be argued that in a parcellation the size of the ROIs determines the minimum spatial resolution for the detection of a hub, but the use of a parcellation with small volumes would have reduced the statistical power in under-represented brain regions. We therefore chose to use an atlas that previously proved itself to fit the functional connectivity better than artifactual parcellations (Mancuso *et al.*, 2019). Still, choosing a different anatomical atlas might have produced slightly divergent results.

Another limitation concerns the practical unfeasibility to derive from the BrainMap repository data about the medication status of the large database of patients that entered this meta-analysis. Moreover, our search did not differentiate between gender and age. Therefore, analyses were unable to evaluate the effects of such variables on measuring the mean physical distance of co-alterations. Given the effect of some psychotropic drug of GM volume (Navari and Dazzan, 2009; Hafeman *et al.*, 2012), and that age and sex have been recently reported to be associated with asymmetries in cortical thickness (Guadalupe *et al.*, 2017; Kong *et al.*, 2018), it could be worth investigating how the symmetry of the

maps of mean physical distance of co-alterations related to GM increases and GM decreases can differ with respect to these variables.

Finally, we calculated the distance between two areas considering the length of the straight line connecting their centroids, but due to curvilinear anatomical constraints the real axonal path linking them is supposed to be probably longer. Moreover, the structural connection between two regions could be indirect, so that the topological distance too could have been useful to provide information about their proximity. However, we were mostly interested in observing whether or not areas are co-altered with far away regions (e.g. if a frontal area is co-altered only with the frontal cortex or even with regions of different lobes). From this perspective, the accurate estimation of the length of the path connecting two regions is not particularly important, though it could be valuable for the transneuronal spread hypothesis.

Conclusion

This study provides the maps of the regions characterized by long mean physical distance of co-alterations related to both GM decreases and GM increases. Our approach has produced four important findings for the understanding of brain diseases. First, when the brain is affected by a pathological process, the anterior and dorsal PFC tend to be involved in a network of long-distance co-alterations, and thus they are to be considered as key hubs of pathology. Second, areas of the left hemisphere seem to be prevalently co-altered in GM decreases, while areas of the right hemisphere appear to be more co-altered in GM increases. This suggests that the two sides of the brain are differently affected by pathological processes. Third, on the basis of the analyses of schizophrenia and Alzheimer's disease, we have found that the measurement of the mean physical distance between co-alterations is able identify the areas that are clinically relevant for the diseases. Lastly, hubs of long-distance co-alteration are similar to those of functional connectivity DC, suggesting a relation between co-alteration and normative connectivity. The mean physical distance of co-alteration, therefore, proves itself to be a useful index capable of

providing new insights into the distribution patterns of morphological alterations caused by brain disorders.

Funding

This study was supported by Fondazione Sanpaolo, Turin (Cauda F. PI).

Competing interest

The authors declare no competing interest.

References

Achard S, Salvador R, Whitcher B, Suckling J, Bullmore E. A Resilient, Low-Frequency, Small-World Human Brain Functional Network with Highly Connected Association Cortical Hubs. J Neurosci 2006; 26: 63–72.

Ahmed RM, Devenney EM, Irish M, Ittner A, Naismith S, Ittner LM, et al. Neuronal network disintegration: Common pathways linking neurodegenerative diseases. J Neurol Neurosurg Psychiatry 2016; 87: 1234–1241.

Alexander-Bloch AF, Vértes PE, Stidd R, Lalonde F, Clasen L, Rapoport J, et al. The anatomical distance of functional connections predicts brain network topology in health and schizophrenia. Cereb Cortex 2013; 23: 127–138.

Andrews-Hanna JR, Reidler JS, Sepulcre J, Poulin R, Buckner RL. Functional-Anatomic Fractionation of the Brain's Default Network. Neuron 2010; 65: 550–562.

Bassett DS, Bullmore E, Verchinski BA, Mattay VS, Weinberger DR, Meyer-Lindenberg A. Hierarchical Organization of Human Cortical Networks in Health and Schizophrenia. J Neurosci 2008; 28: 9239–9248.

Blöchl A, Thoenen H. Characterization of Nerve Growth Factor (NGF) Release from Hippocampal Neurons: Evidence for a Constitutive and an Unconventional Sodium-dependent Regulated Pathway. Eur J Neurosci 1995; 7: 1220–1228.

Braak H, Braak E, Bohl J. Staging of Alzheimer-Related Cortical Destruction. Eur Neurol 1993; 33: 403–408.

Buckholtz JW, Meyer-Lindenberg A. Psychopathology and the Human Connectome: Toward a Transdiagnostic Model of Risk For Mental Illness. Neuron 2012; 74: 990–1004.

Buckner RL. Molecular, Structural, and Functional Characterization of Alzheimer's Disease: Evidence for a Relationship between Default Activity, Amyloid, and Memory. J Neurosci 2005; 25: 7709–7717.

Buckner RL, Andrews-Hanna JR, Schacter DL. The brain's default network: Anatomy, function, and relevance to disease. Ann N Y Acad Sci 2008; 1124: 1–38.

Buckner RL, Sepulcre J, Talukdar T, Krienen FM, Liu H, Hedden T, et al. Cortical Hubs Revealed by Intrinsic Functional Connectivity: Mapping, Assessment of Stability, and Relation to Alzheimer's Disease. J Neurosci 2009; 29: 1860–1873.

Bullmore E, Sporns O. The economy of brain network organization. Nat Rev Neurosci 2012; 13: 336–349.

Cauda F, Costa T, Nani A, Fava L, Palermo S, Bianco F, et al. Are schizophrenia, autistic, and obsessive spectrum disorders dissociable on the basis of neuroimaging morphological findings?: A voxel-based meta-analysis. Autism Res 2017; 10: 1079–1095.

Cauda F, Costa T, Palermo S, D'Agata F, Diano M, Bianco F, et al. Concordance of white matter and gray matter abnormalities in autism spectrum disorders: A voxel-based meta-analysis study. Hum Brain Mapp 2014; 35: 2073–2098.

Cauda F, Mancuso L, Nani A, Costa T. Heterogeneous neuroimaging findings, damage propagation and connectivity: an integrative view. Brain 2019; 142: 1–3.

Cauda F, Nani A, Costa T, Palermo S, Tatu K, Manuello J, et al. The morphometric co-atrophy networking of schizophrenia, autistic and obsessive spectrum disorders. Hum Brain Mapp 2018; 39: 1898–1928.

Cauda F, Nani A, Manuello J, Premi E, Palermo S, Tatu K, et al. Brain structural alterations are distributed following functional, anatomic and genetic connectivity. Brain 2018; 141: 3211–3232.

Chao M V. Neurotrophins and their receptors: A convergence point for many signalling pathways. Nat Rev Neurosci 2003; 4: 299–309.

Crossley NA, Mechelli A, Scott J, Carletti F, Fox PT, Mcguire P, et al. The hubs of the human connectome are generally implicated in the anatomy of brain disorders. Brain 2014; 137: 2382–2395.

Dahoun T, Trossbach S V., Brandon NJ, Korth C, Howes OD. The impact of Disrupted-in-Schizophrenia 1 (DISC1) on the dopaminergic system: A systematic review. Transl Psychiatry 2017; 7: e1015-15.

Diaz-De-Grenu LZ, Acosta-Cabronero J, Chong YFV, Pereira JMS, Sajjadi SA, Williams GB, et al. A brief history of voxel-based grey matter analysis in Alzheimer's disease. J Alzheimer's Dis 2014; 38: 647–659.

Eickhoff S, Laird A, Grefkes C, Wang LE, Zilles K, Fox PT. Coordinate-based ALE meta-analysis of neuroimaging data: a random-effects approach based on empirical estimates of spatial uncertainty. Hum Brain Mapp 2009; 30: 2907–2926.

Eickhoff SB, Bzdok D, Laird AR, Kurth F, Fox PT. Activation likelihood estimation revisited. Neuroimage 2012; 59: 2349–2361.

Esfahlani FZ, Bertolero M, Bassett D, Betzel R. Space-independent community and hub structure of functional brain networks. bioRxiv 2019: 590935.

Evans AC. Networks of anatomical covariance. Neuroimage 2013; 80: 489–504.

Fornito A, Zalesky A, Breakspear M. The connectomics of brain disorders. Nat Rev Neurosci 2015; 16: 159–172.

Fox PT, Laird AR, Fox SP, Fox PM, Uecker AM, Crank M, et al. BrainMap taxonomy of experimental design: Description and evaluation. Hum Brain Mapp 2005; 25: 185–198.

Fox PT, Lancaster JL. Mapping context and content: The BrainMap model. Nat Rev Neurosci 2002; 3: 319–321.

Gall CM, Isackson PJ. Limbic seizures increase neuronal production of messenger RNA for nerve growth factor. Science (80-) 1989

García-Martí G, Aguilar EJ, Lull JJ, Martí-Bonmatí L, Escartí MJ, Manjón J V., et al. Schizophrenia with auditory hallucinations: A voxel-based morphometry study. Prog Neuro-Psychopharmacology Biol Psychiatry 2008; 32: 72–80.

Goedert M, Masuda-Suzukake M, Falcon B. Like prions: The propagation of aggregated tau and α-synuclein in neurodegeneration. Brain 2017; 140: 266–278.

Goodkind M, Eickhoff SB, Oathes DJ, Jiang Y, Chang A, Jones-Hagata LB, et al. Identification of a common neurobiological substrate for mental Illness. JAMA Psychiatry 2015; 72: 305–315.

Green S, Higgins JP, Alderson P, Clarke M, Mulrow CD, Oxman AD. Introduction. In: Higgins JP, Green S, editor(s). Cochrane Handbook for Systematic Reviews of Interventions. Chichester, UK: John Wiley & Sons, Ltd; 2008. p. 1–9

Guadalupe T, Mathias SR, vanErp TGM, Whelan CD, Zwiers MP, Abe Y, et al. Human subcortical brain asymmetries in 15,847 people worldwide reveal effects of age and sex. Brain Imaging Behav 2017; 11: 1497–1514.

Guest WC, Silverman JM, Pokrishevsky E, O'Neill MA, Grad LI, Cashman NR. Generalization of the Prion Hypothesis to Other Neurodegenerative Diseases: An Imperfect Fit. J Toxicol Environ Heal Part A 2011; 74: 1433–1459.

de Haan W, Mott K, van Straaten ECW, Scheltens P, Stam CJ. Activity Dependent Degeneration Explains Hub Vulnerability in Alzheimer's Disease. PLoS Comput Biol 2012; 8

Hafeman DM, Chang KD, Garrett AS, Sanders EM, Phillips ML. Effects of medication on neuroimaging findings in bipolar disorder: An updated review. Bipolar Disord 2012; 14: 375–410.

He Y, Chen ZJ, Evans AC. Small-world anatomical networks in the human brain revealed by cortical thickness from MRI. Cereb Cortex 2007; 17: 2407–2419.

Iturria-Medina Y, Sotero RC, Toussaint PJ, Evans AC. Epidemic Spreading Model to Characterize Misfolded Proteins Propagation in Aging and Associated Neurodegenerative Disorders. PLoS Comput Biol 2014; 10

Janke AL, De Zubicaray G, Rose SE, Griffin M, Chalk JB, Galloway GJ. 4D deformation

modeling of cortical disease progression in Alzheimer's dementia. Magn Reson Med 2001; 46: 661–666.

Kapur S. Psychosis as a state of aberrant salience: A framework linking biology, phenomenology, and pharmacology in schizophrenia. Am J Psychiatry 2003; 160: 13–23.

Kohara K, Kitamura A, Morishima M, Tsumoto T. Activity-dependent transfer of brain-derived neurotrophic factor to postsynaptic neurons. Science (80-) 2001; 291: 2419–2423.

Kong X-Z, Mathias SR, Guadalupe T, Glahn DC, Franke B, Crivello F, et al. Mapping cortical brain asymmetry in 17,141 healthy individuals worldwide via the ENIGMA Consortium. Proc Natl Acad Sci 2018; 115: E5154–E5163.

Korth C. Aggregated proteins in schizophrenia and other chronic mental diseases. Prion 2012; 6: 134–141.

Laird AR, Lancaster JL, Fox PT. BrainMap: The Social Evolution of a Human Brain Mapping Database. Neuroinformatics 2005; 3: 065–078.

Lancaster JL, Tordesillas-Gutiérrez D, Martinez M, Salinas F, Evans A, Zilles K, et al. Bias between MNI and Talairach coordinates analyzed using the ICBM-152 brain template. Hum Brain Mapp 2007; 28: 1194–1205.

Lancaster JL, Woldorff MG, Parsons LM, Liotti M, Freitas CS, Rainey L, et al. Automated Talairach Atlas labels for functional brain mapping. Hum Brain Mapp 2000; 10: 120–131.

Laughlin SB, Sejnowski TJ. Communication in neuronal networks. Science (80-) 2003; 301: 1870–1874.

Leliveld SR, Bader V, Hendriks P, Prikulis I, Sajnani G, Requena JR, et al. Insolubility of Disrupted-in-Schizophrenia 1 Disrupts Oligomer-Dependent Interactions with Nuclear Distribution Element 1 and Is Associated with Sporadic Mental Disease. J Neurosci 2008; 28: 3839–3845.

Liao XH, Xia MR, Xu T, Dai ZJ, Cao XY, Niu HJ, et al. Functional brain hubs and their test-

retest reliability: A multiband resting-state functional MRI study. Neuroimage 2013; 83: 969–982.

Liberati A, Altman DG, Tetzlaff J, Mulrow C, Gotzsche PC, Ioannidis JPA, et al. The PRISMA statement for reporting systematic reviews and meta-analyses of studies that evaluate healthcare interventions: explanation and elaboration. BMJ 2009; 339: b2700–b2700.

Liddle EB, Price D, Palaniyappan L, Brookes MJ, Robson SE, Hall EL, et al. Abnormal salience signaling in schizophrenia: The role of integrative beta oscillations. Hum Brain Mapp 2016; 37: 1361–1374.

Loewenstein DA, Barker WW, Chang JY, Apicella A, Yoshii F, Kothari P, et al. Predominant left hemisphere metabolic dysfunction in dementia. Arch Neurol 1989; 46: 146–152.

Mancuso L, Costa T, Nani A, Manuello J, Liloia D, Gelmini G, et al. The homotopic connectivity of the functional brain: a meta-analytic approach. Sci Rep 2019; 9: 3346.

Mandelli ML, Vilaplana E, Brown JA, Hubbard HI, Binney RJ, Attygalle S, et al. Healthy brain connectivity predicts atrophy progression in non-fluent variant of primary progressive aphasia. Brain 2016; 139: 2778–2791.

Manoliu A, Riedl V, Zherdin A, Mühlau M, Schwerthöffer D, Scherr M, et al. Aberrant dependence of default mode/central executive network interactions on anterior insular salience network activity in schizophrenia. Schizophr Bull 2014; 40: 428–437.

Manuello J, Nani A, Premi E, Borroni B, Costa T, Tatu K, et al. The pathoconnectivity profile of Alzheimer's disease: A morphometric coalteration network analysis. Front Neurol 2018; 8: 1–15.

McTeague LM, Goodkind MS, Etkin A. Transdiagnostic impairment of cognitive control in mental illness. J Psychiatr Res 2016; 83: 37–46.

Modinos G, Vercammen A, Mechelli A, Knegtering H, McGuire PK, Aleman A. Structural

covariance in the hallucinating brain: A voxel-based morphometry study. J Psychiatry Neurosci 2009; 34: 465–469.

Moher D, Liberati A, Tetzlaff J, Altman DG. Preferred Reporting Items for Systematic Reviews and Meta-Analyses: The PRISMA Statement. J Clin Epidemiol 2009; 62: 1006–1012.

Navari S, Dazzan P. Do antipsychotic drugs affect brain structure? A systematic and critical review of MRI findings. Psychol Med 2009; 39: 1763–1777.

Neckelmann G, Specht K, Lund A, Ersland L, Smievoll AI, Neckelmann D, et al. MR morphometry analysis of grey matter volume reduction in schizophrenia: Association with hallucinations. Int J Neurosci 2006; 116: 9–23.

Okada N, Fukunaga M, Yamashita F, Koshiyama D, Yamamori H, Ohi K, et al. Abnormal asymmetries in subcortical brain volume in schizophrenia. Mol Psychiatry 2016; 21: 1460–1466.

Palaniyappan L, Liddle PF. Does the salience network play a cardinal role in psychosis? An emerging hypothesis of insular dysfunction. J Psychiatry Neurosci 2012; 37: 17–27.

Palaniyappan L, White TP, Liddle PF. The Concept of Salience Network Dysfunction in Schizophrenia: From Neuroimaging Observations to Therapeutic Opportunities. Curr Top Med Chem 2013; 12: 2324–2338.

Patel RS, Bowman FD, Rilling JK. A Bayesian approach to determining connectivity of the human brain. Hum Brain Mapp 2006; 27: 267–276.

Perlson E, Maday S, Fu M meng, Moughamian AJ, Holzbaur ELF. Retrograde axonal transport: Pathways to cell death? Trends Neurosci 2010; 33: 335–344.

Pievani M, de Haan W, Wu T, Seeley WW, Frisoni GB. Functional network disruption in the degenerative dementias. Lancet Neurol 2011; 10: 829–843.

Plaze M, Bartrés-Faz D, Martinot JL, Januel D, Bellivier F, De Beaurepaire R, et al. Left

superior temporal gyrus activation during sentence perception negatively correlates with auditory hallucination severity in schizophrenia patients. Schizophr Res 2006; 87: 109–115.

Raj A, Kuceyeski A, Weiner M. A Network Diffusion Model of Disease Progression in Dementia. Neuron 2012; 73: 1204–1215.

Rubinov M, Sporns O. Complex network measures of brain connectivity: Uses and interpretations. Neuroimage 2010; 52: 1059–1069.

Saxena S, Caroni P. Selective Neuronal Vulnerability in Neurodegenerative Diseases: From Stressor Thresholds to Degeneration. Neuron 2011; 71: 35–48.

Scarpazza C, Tognin S, Frisciata S, Sartori G, Mechelli A. False positive rates in Voxel-based Morphometry studies of the human brain: Should we be worried? Neurosci Biobehav Rev 2015; 52: 49–55.

Seeley WW, Crawford RK, Zhou J, Miller BL, Greicius MD. Neurodegenerative Diseases Target Large-Scale Human Brain Networks. Neuron 2009; 62: 42–52.

Sepulcre J, Liu H, Talukdar T, Martincorena I, Thomas Yeo BT, Buckner RL. The organization of local and distant functional connectivity in the human brain. PLoS Comput Biol 2010; 6: 1–15.

Sheline YI, Barch DM, Price JL, Rundle MM, Vaishnavi SN, Snyder AZ, et al. The default mode network and self-referential processes in depression. Proc Natl Acad Sci 2009; 106: 1942–1947.

Sporns O, Zwi JD. The Small World of the Cerebral Cortex. Neuroinformatics 2004; 2: 145–162.

Tatu K, Costa T, Nani A, Diano M, Quarta DG, Duca S, et al. How do morphological alterations caused by chronic pain distribute across the brain? A meta-analytic co-alteration study. NeuroImage Clin 2018; 18: 15–30.

Thompson PM, Hayashi KM, Dutton RA, Chiang M-C, Leow AD, SowellL ER, et al.

Tracking Alzheimer's Disease. Ann N Y Acad Sci 2007; 1097: 183–214.

Thompson PM, Hayashi KM, de Zubicaray G, Janke AL, Rose SE, Semple J, et al. Dynamics of Gray Matter Loss in Alzheimer's Disease. J Neurosci 2003; 23: 994–1005.

Thompson PM, Mega MS, Woods RP, Zoumalan CI, Lindshield CJ, Blanton RE, et al. Cortical Change in Alzheimer's Disease Detected with a Disease-specific Population-based Brain Atlas. Cereb Cortex 2001; 11: 1–16.

Tropea D, Hardingham N, Millar K, Fox K. Mechanisms underlying the role of DISC1 in synaptic plasticity. J Physiol 2018; 596: 2747–2771.

Trossbach S V., Bader V, Hecher L, Pum ME, Masoud ST, Prikulis I, et al. Misassembly of full-length Disrupted-in-Schizophrenia 1 protein is linked to altered dopamine homeostasis and behavioral deficits. Mol Psychiatry 2016; 21: 1561–1572.

Turkeltaub PE, Eickhoff SB, Laird AR, Fox M, Wiener M, Fox P. Minimizing within-experiment and within-group effects in activation likelihood estimation meta-analyses. Hum Brain Mapp 2012; 33: 1–13.

Uddin LQ. Salience processing and insular cortical function and dysfunction. In: Nature Reviews Neuroscience. Nature Publishing Group; 2015. p. 55–61

Vanasse TJ, Fox PM, Barron DS, Robertson M, Eickhoff SB, Lancaster JL, et al. BrainMap VBM: An environment for structural meta-analysis. Hum Brain Mapp 2018; 39: 3308–3325.

Warren JD, Rohrer JD, Hardy J. Disintegrating Brain Networks: From Syndromes to Molecular Nexopathies. Neuron 2012; 73: 1060–1062.

Warren JD, Rohrer JD, Schott JM, Fox NC, Hardy J, Rossor MN. Molecular nexopathies: a new paradigm of neurodegenerative disease. Trends Neurosci 2013; 36: 561–569.

Watts DJ, Strogatz SH, Tseng Y-M. Collective dynamics of 'small-world' networks. Nature 1998; 153: 810–817.

Wheeler AL, Felsky D, Viviano JD, Stojanovski S, Ameis SH, Szatmari P, et al. BDNF-

Dependent Effects on Amygdala–Cortical Circuitry and Depression Risk in Children and Youth. Cereb Cortex 2017; 28: 1760–1770.

Wheeler AL, Wessa M, Szeszko PR, Foussias G, Chakravarty MM, Lerch JP, et al. Further neuroimaging evidence for the deficit subtype of schizophrenia: A cortical connectomics analysis. JAMA Psychiatry 2015; 72: 446–455.

White TP, Joseph V, Francis ST, Liddle PF. Aberrant salience network (bilateral insula and anterior cingulate cortex) connectivity during information processing in schizophrenia. Schizophr Res 2010; 123: 105–115.

World Health Organisation. The ICD-10 classification of mental and behavioural disorders: clinical descriptions and diagnostic guidelines. World Heal Organ 1992

Zhou J, Gennatas ED, Kramer JH, Miller BL, Seeley WW. Predicting Regional Neurodegeneration from the Healthy Brain Functional Connectome. Neuron 2012; 73: 1216–1227.

Zhu S, Abounit S, Korth C, Zurzolo C. Transfer of disrupted-in-schizophrenia 1 aggregates between neuronal-like cells occurs in tunnelling nanotubes and is promoted by dopamine. Open Biol 2017; 7

Ahmed RM, Devenney EM, Irish M, Ittner A, Naismith S, Ittner LM, et al. Neuronal network disintegration: Common pathways linking neurodegenerative diseases. J Neurol Neurosurg Psychiatry 2016; 87: 1234–1241.

Alexander-Bloch AF, Vértes PE, Stidd R, Lalonde F, Clasen L, Rapoport J, et al. The anatomical distance of functional connections predicts brain network topology in health and schizophrenia. Cereb Cortex 2013; 23: 127–138.

Andrews-Hanna JR, Reidler JS, Sepulcre J, Poulin R, Buckner RL. Functional-Anatomic Fractionation of the Brain's Default Network. Neuron 2010; 65: 550–562.

Bassett DS, Bullmore E, Verchinski BA, Mattay VS, Weinberger DR, Meyer-Lindenberg A. Hierarchical Organization of Human Cortical Networks in Health and Schizophrenia. J Neurosci 2008; 28: 9239–9248.

Braak H, Braak E, Bohl J. Staging of Alzheimer-Related Cortical Destruction. Eur Neurol 1993; 33: 403–408.

Buckholtz JW, Meyer-Lindenberg A. Psychopathology and the Human Connectome: Toward a Transdiagnostic Model of Risk For Mental Illness. Neuron 2012; 74: 990–1004.

Buckner RL. Molecular, Structural, and Functional Characterization of Alzheimer's Disease: Evidence for a Relationship between Default Activity, Amyloid, and Memory. J Neurosci 2005; 25: 7709–7717.

Buckner RL, Andrews-Hanna JR, Schacter DL. The brain's default network: Anatomy, function, and relevance to disease. Ann N Y Acad Sci 2008; 1124: 1–38.

Buckner RL, Sepulcre J, Talukdar T, Krienen FM, Liu H, Hedden T, et al. Cortical Hubs Revealed by Intrinsic Functional Connectivity: Mapping, Assessment of Stability, and Relation to Alzheimer's Disease. J Neurosci 2009; 29: 1860–1873.

Bullmore E, Sporns O. The economy of brain network organization. Nat Rev Neurosci 2012; 13: 336–349.

Cauda F, Costa T, Nani A, Fava L, Palermo S, Bianco F, et al. Are schizophrenia, autistic, and obsessive spectrum disorders dissociable on the basis of neuroimaging morphological findings?: A voxel-based meta-analysis. Autism Res 2017; 10: 1079–1095.

Cauda F, Costa T, Palermo S, D'Agata F, Diano M, Bianco F, et al. Concordance of white matter and gray matter abnormalities in autism spectrum disorders: A voxel-based meta-analysis study. Hum Brain Mapp 2014; 35: 2073–2098.

Cauda F, Nani A, Costa T, Palermo S, Tatu K, Manuello J, et al. The morphometric co-atrophy networking of schizophrenia, autistic and obsessive spectrum disorders. Hum Brain Mapp 2018; 39: 1898–1928.

Cauda F, Nani A, Manuello J, Premi E, Palermo S, Tatu K, et al. Brain structural alterations are distributed following functional, anatomic and genetic connectivity. Brain 2018; 141: 3211–3232.

Crossley NA, Mechelli A, Scott J, Carletti F, Fox PT, Mcguire P, et al. The hubs of the human connectome are generally implicated in the anatomy of brain disorders. Brain 2014; 137: 2382–2395.

Dahoun T, Trossbach S V., Brandon NJ, Korth C, Howes OD. The impact of Disrupted-in-Schizophrenia 1 (DISC1) on the dopaminergic system: A systematic review. Transl Psychiatry 2017; 7: e1015-15.

Diaz-De-Grenu LZ, Acosta-Cabronero J, Chong YFV, Pereira JMS, Sajjadi SA, Williams GB, et al. A brief history of voxel-based grey matter analysis in Alzheimer's disease. J Alzheimer's Dis 2014; 38: 647–659.

Eickhoff S, Laird A, Grefkes C, Wang LE, Zilles K, Fox PT. Coordinate-based ALE meta-analysis of neuroimaging data: a random-effects approach based on empirical estimates of spatial uncertainty. Hum Brain Mapp 2009; 30: 2907–2926.

Eickhoff SB, Bzdok D, Laird AR, Kurth F, Fox PT. Activation likelihood estimation revisited. Neuroimage 2012; 59: 2349–2361.

Eickhoff SB, Nichols TE, Laird AR, Hoffstaedter F, Amunts K, Fox PT, et al. Behavior, sensitivity, and power of activation likelihood estimation characterized by massive empirical simulation. Neuroimage 2016; 137: 70–85.

Esfahlani FZ, Bertolero M, Bassett D, Betzel R. Space-independent community and hub structure of functional brain networks. bioRxiv 2019: 590935.

Evans AC. Networks of anatomical covariance. Neuroimage 2013; 80: 489–504.

Fornito A, Zalesky A, Breakspear M. The connectomics of brain disorders. Nat Rev Neurosci 2015; 16: 159–172.

Fox PT, Laird AR, Fox SP, Fox PM, Uecker AM, Crank M, et al. BrainMap taxonomy of experimental design: Description and evaluation. Hum Brain Mapp 2005; 25: 185–198.

Fox PT, Lancaster JL. Mapping context and content: The BrainMap model. Nat Rev Neurosci 2002; 3: 319–321.

García-Martí G, Aguilar EJ, Lull JJ, Martí-Bonmatí L, Escartí MJ, Manjón J V., et al. Schizophrenia with auditory hallucinations: A voxel-based morphometry study. Prog Neuro-Psychopharmacology Biol Psychiatry 2008; 32: 72–80.

Goedert M, Masuda-Suzukake M, Falcon B. Like prions: The propagation of aggregated tau and α-synuclein in neurodegeneration. Brain 2017; 140: 266–278.

Goodkind M, Eickhoff SB, Oathes DJ, Jiang Y, Chang A, Jones-Hagata LB, et al. Identification of a common neurobiological substrate for mental Illness. JAMA Psychiatry 2015; 72: 305–315.

Green S, Higgins JP, Alderson P, Clarke M, Mulrow CD, Oxman AD. Introduction. In: Higgins JP, Green S, editor(s). Cochrane Handbook for Systematic Reviews of Interventions. Chichester, UK: John Wiley & Sons, Ltd; 2008. p. 1–9

Guadalupe T, Mathias SR, vanErp TGM, Whelan CD, Zwiers MP, Abe Y, et al. Human subcortical brain asymmetries in 15,847 people worldwide reveal effects of age and sex. Brain Imaging Behav 2017; 11: 1497–1514.

Guest WC, Silverman JM, Pokrishevsky E, O'Neill MA, Grad LI, Cashman NR. Generalization of the Prion Hypothesis to Other Neurodegenerative Diseases: An Imperfect Fit. J Toxicol Environ Heal Part A 2011; 74: 1433–1459.

de Haan W, Mott K, van Straaten ECW, Scheltens P, Stam CJ. Activity Dependent Degeneration Explains Hub Vulnerability in Alzheimer's Disease. PLoS Comput Biol 2012; 8

He Y, Chen ZJ, Evans AC. Small-world anatomical networks in the human brain revealed by cortical thickness from MRI. Cereb Cortex 2007; 17: 2407–2419.

Iturria-Medina Y, Sotero RC, Toussaint PJ, Evans AC. Epidemic Spreading Model to Characterize Misfolded Proteins Propagation in Aging and Associated Neurodegenerative Disorders. PLoS Comput Biol 2014; 10

Janke AL, De Zubicaray G, Rose SE, Griffin M, Chalk JB, Galloway GJ. 4D deformation modeling of cortical disease progression in Alzheimer's dementia. Magn Reson Med 2001; 46: 661–666.

Kapur S. Psychosis as a state of aberrant salience: A framework linking biology, phenomenology, and pharmacology in schizophrenia. Am J Psychiatry 2003; 160: 13–23.

Kong X-Z, Mathias SR, Guadalupe T, Glahn DC, Franke B, Crivello F, et al. Mapping cortical brain asymmetry in 17,141 healthy individuals worldwide via the ENIGMA Consortium. Proc Natl Acad Sci 2018; 115: E5154–E5163.

Korth C. Aggregated proteins in schizophrenia and other chronic mental diseases. Prion 2012; 6: 134–141.

Laird AR, Lancaster JL, Fox PT. BrainMap: The Social Evolution of a Human Brain Mapping Database. Neuroinformatics 2005; 3: 065–078.

Lancaster JL, Tordesillas-Gutiérrez D, Martinez M, Salinas F, Evans A, Zilles K, et al. Bias between MNI and Talairach coordinates analyzed using the ICBM-152 brain template. Hum Brain Mapp 2007; 28: 1194–1205.

Lancaster JL, Woldorff MG, Parsons LM, Liotti M, Freitas CS, Rainey L, et al. Automated Talairach Atlas labels for functional brain mapping. Hum Brain Mapp 2000; 10: 120–131.

Laughlin SB, Sejnowski TJ. Communication in neuronal networks. Science (80-) 2003; 301: 1870–1874.

Leliveld SR, Bader V, Hendriks P, Prikulis I, Sajnani G, Requena JR, et al. Insolubility of Disrupted-in-Schizophrenia 1 Disrupts Oligomer-Dependent Interactions with Nuclear Distribution Element 1 and Is Associated with Sporadic Mental Disease. J Neurosci 2008; 28: 3839–3845.

Liao XH, Xia MR, Xu T, Dai ZJ, Cao XY, Niu HJ, et al. Functional brain hubs and their test-retest reliability: A multiband resting-state functional MRI study. Neuroimage 2013; 83: 969–982.

Liberati A, Altman DG, Tetzlaff J, Mulrow C, Gotzsche PC, Ioannidis JPA, et al. The PRISMA statement for reporting systematic reviews and meta-analyses of studies that evaluate healthcare interventions: explanation and elaboration. BMJ 2009; 339: b2700–b2700.

Liddle EB, Price D, Palaniyappan L, Brookes MJ, Robson SE, Hall EL, et al. Abnormal salience signaling in schizophrenia: The role of integrative beta oscillations. Hum Brain Mapp 2016; 37: 1361–1374.

Loewenstein DA, Barker WW, Chang JY, Apicella A, Yoshii F, Kothari P, et al. Predominant left hemisphere metabolic dysfunction in dementia. Arch Neurol 1989; 46: 146–152.

Mancuso L, Costa T, Nani A, Manuello J, Liloia D, Gelmini G, et al. The homotopic connectivity of the functional brain: a meta-analytic approach. Sci Rep 2019; 9: 3346.

Mandelli ML, Vilaplana E, Brown JA, Hubbard HI, Binney RJ, Attygalle S, et al. Healthy brain connectivity predicts atrophy progression in non-fluent variant of primary progressive aphasia. Brain 2016; 139: 2778–2791.

Manoliu A, Riedl V, Zherdin A, Mühlau M, Schwerthöffer D, Scherr M, et al. Aberrant dependence of default mode/central executive network interactions on anterior insular salience network activity in schizophrenia. Schizophr Bull 2014; 40: 428–437.

Manuello J, Nani A, Premi E, Borroni B, Costa T, Tatu K, et al. The pathoconnectivity profile of Alzheimer's disease: A morphometric coalteration network analysis. Front Neurol 2018; 8: 1–15.

McTeague LM, Goodkind MS, Etkin A. Transdiagnostic impairment of cognitive control in mental illness. J Psychiatr Res 2016; 83: 37–46.

Modinos G, Vercammen A, Mechelli A, Knegtering H, McGuire PK, Aleman A. Structural covariance in the hallucinating brain: A voxel-based morphometry study. J Psychiatry Neurosci 2009; 34: 465–469.

Moher D, Liberati A, Tetzlaff J, Altman DG. Preferred Reporting Items for Systematic Reviews and Meta-Analyses: The PRISMA Statement. J Clin Epidemiol 2009; 62: 1006–1012.

Neckelmann G, Specht K, Lund A, Ersland L, Smievoll AI, Neckelmann D, et al. MR morphometry analysis of grey matter volume reduction in schizophrenia: Association with hallucinations. Int J Neurosci 2006; 116: 9–23.

Okada N, Fukunaga M, Yamashita F, Koshiyama D, Yamamori H, Ohi K, et al. Abnormal asymmetries in subcortical brain volume in schizophrenia. Mol Psychiatry 2016; 21: 1460–1466.

Palaniyappan L, Liddle PF. Does the salience network play a cardinal role in psychosis? An emerging hypothesis of insular dysfunction. J Psychiatry Neurosci 2012; 37: 17–27.

Palaniyappan L, White TP, Liddle PF. The Concept of Salience Network Dysfunction in Schizophrenia: From Neuroimaging Observations to Therapeutic Opportunities. Curr Top Med Chem 2013; 12: 2324–2338.

Patel RS, Bowman FD, Rilling JK. A Bayesian approach to determining connectivity of the human brain. Hum Brain Mapp 2006; 27: 267–276.

Pievani M, de Haan W, Wu T, Seeley WW, Frisoni GB. Functional network disruption in the degenerative dementias. Lancet Neurol 2011; 10: 829–843.

Plaze M, Bartrés-Faz D, Martinot JL, Januel D, Bellivier F, De Beaurepaire R, et al. Left superior temporal gyrus activation during sentence perception negatively correlates with auditory hallucination severity in schizophrenia patients. Schizophr Res 2006; 87: 109–115.

Raj A, Kuceyeski A, Weiner M. A Network Diffusion Model of Disease Progression in Dementia. Neuron 2012; 73: 1204–1215.

Rubinov M, Sporns O. Complex network measures of brain connectivity: Uses and interpretations. Neuroimage 2010; 52: 1059–1069.

Saxena S, Caroni P. Selective Neuronal Vulnerability in Neurodegenerative Diseases: From Stressor Thresholds to Degeneration. Neuron 2011; 71: 35–48.

Scarpazza C, Tognin S, Frisciata S, Sartori G, Mechelli A. False positive rates in Voxel-based Morphometry studies of the human brain: Should we be worried? Neurosci Biobehav Rev 2015; 52: 49–55.

Seeley WW, Crawford RK, Zhou J, Miller BL, Greicius MD. Neurodegenerative Diseases Target Large-Scale Human Brain Networks. Neuron 2009; 62: 42–52.

Sepulcre J, Liu H, Talukdar T, Martincorena I, Thomas Yeo BT, Buckner RL. The organization of local and distant functional connectivity in the human brain. PLoS Comput Biol 2010; 6: 1–15.

Sheline YI, Barch DM, Price JL, Rundle MM, Vaishnavi SN, Snyder AZ, et al. The default mode network and self-referential processes in depression. Proc Natl Acad Sci 2009; 106: 1942–1947.

Sporns O, Zwi JD. The Small World of the Cerebral Cortex. Neuroinformatics 2004; 2: 145–162.

Tatu K, Costa T, Nani A, Diano M, Quarta DG, Duca S, et al. How do morphological alterations caused by chronic pain distribute across the brain? A meta-analytic co-alteration study. NeuroImage Clin 2018; 18: 15–30.

Thompson PM, Hayashi KM, Dutton RA, Chiang M-C, Leow AD, SowellL ER, et al. Tracking Alzheimer's Disease. Ann N Y Acad Sci 2007; 1097: 183–214.

Thompson PM, Hayashi KM, de Zubicaray G, Janke AL, Rose SE, Semple J, et al. Dynamics of Gray Matter Loss in Alzheimer's Disease. J Neurosci 2003; 23: 994–1005.

Thompson PM, Mega MS, Woods RP, Zoumalan CI, Lindshield CJ, Blanton RE, et al.

Cortical Change in Alzheimer's Disease Detected with a Disease-specific Population-based Brain Atlas. Cereb Cortex 2001; 11: 1–16.

Tropea D, Hardingham N, Millar K, Fox K. Mechanisms underlying the role of DISC1 in synaptic plasticity. J Physiol 2018; 596: 2747–2771.

Trossbach S V., Bader V, Hecher L, Pum ME, Masoud ST, Prikulis I, et al. Misassembly of full-length Disrupted-in-Schizophrenia 1 protein is linked to altered dopamine homeostasis and behavioral deficits. Mol Psychiatry 2016; 21: 1561–1572.

Turkeltaub PE, Eickhoff SB, Laird AR, Fox M, Wiener M, Fox P. Minimizing within-experiment and within-group effects in activation likelihood estimation meta-analyses. Hum Brain Mapp 2012; 33: 1–13.

Uddin LQ. Salience processing and insular cortical function and dysfunction. In: Nature Reviews Neuroscience. Nature Publishing Group; 2015. p. 55–61

Vanasse TJ, Fox PM, Barron DS, Robertson M, Eickhoff SB, Lancaster JL, et al. BrainMap VBM: An environment for structural meta-analysis. Hum Brain Mapp 2018; 39: 3308–3325.

Warren JD, Rohrer JD, Hardy J. Disintegrating Brain Networks: From Syndromes to Molecular Nexopathies. Neuron 2012; 73: 1060–1062.

Warren JD, Rohrer JD, Schott JM, Fox NC, Hardy J, Rossor MN. Molecular nexopathies: a new paradigm of neurodegenerative disease. Trends Neurosci 2013; 36: 561–569.

Watts DJ, Strogatz SH, Tseng Y-M. Collective dynamics of 'small-world' networks. Nature 1998; 153: 810–817.

Wheeler AL, Felsky D, Viviano JD, Stojanovski S, Ameis SH, Szatmari P, et al. BDNF-Dependent Effects on Amygdala–Cortical Circuitry and Depression Risk in Children and Youth. Cereb Cortex 2017; 28: 1760–1770.

Wheeler AL, Wessa M, Szeszko PR, Foussias G, Chakravarty MM, Lerch JP, et al. Further neuroimaging evidence for the deficit subtype of schizophrenia: A cortical connectomics

analysis. JAMA Psychiatry 2015; 72: 446–455.

White TP, Joseph V, Francis ST, Liddle PF. Aberrant salience network (bilateral insula and anterior cingulate cortex) connectivity during information processing in schizophrenia. Schizophr Res 2010; 123: 105–115.

World Health Organisation. The ICD-10 classification of mental and behavioural disorders: clinical descriptions and diagnostic guidelines. World Heal Organ 1992

Zhou J, Gennatas ED, Kramer JH, Miller BL, Seeley WW. Predicting Regional Neurodegeneration from the Healthy Brain Functional Connectome. Neuron 2012; 73: 1216–1227.

Zhu S, Abounit S, Korth C, Zurzolo C. Transfer of disrupted-in-schizophrenia 1 aggregates between neuronal-like cells occurs in tunnelling nanotubes and is promoted by dopamine. Open Biol 2017; 7

Ahmed RM, Devenney EM, Irish M, Ittner A, Naismith S, Ittner LM, et al. Neuronal network disintegration: Common pathways linking neurodegenerative diseases. J. Neurol. Neurosurg. Psychiatry 2016; 87: 1234–1241.

Alexander-Bloch AF, Vértes PE, Stidd R, Lalonde F, Clasen L, Rapoport J, et al. The anatomical distance of functional connections predicts brain network topology in health and schizophrenia. Cereb. Cortex 2013; 23: 127–138.

Andrews-Hanna JR, Reidler JS, Sepulcre J, Poulin R, Buckner RL. Functional-Anatomic Fractionation of the Brain's Default Network. Neuron 2010; 65: 550–562.

Bassett DS, Bullmore E, Verchinski BA, Mattay VS, Weinberger DR, Meyer-Lindenberg A. Hierarchical Organization of Human Cortical Networks in Health and Schizophrenia. J. Neurosci. 2008; 28: 9239–9248.

Braak H, Braak E, Bohl J. Staging of Alzheimer-Related Cortical Destruction. Eur. Neurol.

1993; 33: 403–408.

Buckholtz JW, Meyer-Lindenberg A. Psychopathology and the Human Connectome: Toward a Transdiagnostic Model of Risk For Mental Illness. Neuron 2012; 74: 990–1004.

Buckner RL. Molecular, Structural, and Functional Characterization of Alzheimer's Disease: Evidence for a Relationship between Default Activity, Amyloid, and Memory. J. Neurosci. 2005; 25: 7709–7717.

Buckner RL, Andrews-Hanna JR, Schacter DL. The brain's default network: Anatomy, function, and relevance to disease. Ann. N. Y. Acad. Sci. 2008; 1124: 1–38.

Buckner RL, Sepulcre J, Talukdar T, Krienen FM, Liu H, Hedden T, et al. Cortical Hubs Revealed by Intrinsic Functional Connectivity: Mapping, Assessment of Stability, and Relation to Alzheimer's Disease. J. Neurosci. 2009; 29: 1860–1873.

Bullmore E, Sporns O. The economy of brain network organization. Nat. Rev. Neurosci. 2012; 13: 336–349.

Cauda F, Costa T, Nani A, Fava L, Palermo S, Bianco F, et al. Are schizophrenia, autistic, and obsessive spectrum disorders dissociable on the basis of neuroimaging morphological findings?: A voxel-based meta-analysis. Autism Res. 2017; 10: 1079–1095.

Cauda F, Costa T, Palermo S, D'Agata F, Diano M, Bianco F, et al. Concordance of white matter and gray matter abnormalities in autism spectrum disorders: A voxel-based meta-analysis study. Hum. Brain Mapp. 2014; 35: 2073–2098.

Cauda F, Nani A, Costa T, Palermo S, Tatu K, Manuello J, et al. The morphometric co-atrophy networking of schizophrenia, autistic and obsessive spectrum disorders. Hum. Brain Mapp. 2018a; 39: 1898–1928.

Cauda F, Nani A, Manuello J, Premi E, Palermo S, Tatu K, et al. Brain structural alterations are distributed following functional, anatomic and genetic connectivity. Brain 2018b; 141: 3211–3232.

Crossley NA, Mechelli A, Scott J, Carletti F, Fox PT, Mcguire P, et al. The hubs of the human connectome are generally implicated in the anatomy of brain disorders. Brain 2014; 137: 2382–2395.

Eickhoff S, Laird A, Grefkes C, Wang LE, Zilles K, Fox PT. Coordinate-based ALE meta-analysis of neuroimaging data: a random-effects approach based on empirical estimates of spatial uncertainty. Hum. Brain Mapp. 2009; 30: 2907–2926.

Eickhoff SB, Bzdok D, Laird AR, Kurth F, Fox PT. Activation likelihood estimation revisited. Neuroimage 2012; 59: 2349–2361.

Eickhoff SB, Nichols TE, Laird AR, Hoffstaedter F, Amunts K, Fox PT, et al. Behavior, sensitivity, and power of activation likelihood estimation characterized by massive empirical simulation. Neuroimage 2016; 137: 70–85.

Esfahlani FZ, Bertolero M, Bassett D, Betzel R. Space-independent community and hub structure of functional brain networks. bioRxiv 2019: 590935.

Evans AC. Networks of anatomical covariance. Neuroimage 2013; 80: 489–504.

Fornito A, Zalesky A, Breakspear M. The connectomics of brain disorders. Nat. Rev. Neurosci. 2015; 16: 159–172.

Fox PT, Laird AR, Fox SP, Fox PM, Uecker AM, Crank M, et al. BrainMap taxonomy of experimental design: Description and evaluation. Hum. Brain Mapp. 2005; 25: 185–198.

Fox PT, Lancaster JL. Mapping context and content: The BrainMap model. Nat. Rev. Neurosci. 2002; 3: 319–321.

García-Martí G, Aguilar EJ, Lull JJ, Martí-Bonmatí L, Escartí MJ, Manjón J V., et al. Schizophrenia with auditory hallucinations: A voxel-based morphometry study. Prog. Neuro-Psychopharmacology Biol. Psychiatry 2008; 32: 72–80.

Goedert M, Masuda-Suzukake M, Falcon B. Like prions: The propagation of aggregated tau and α-synuclein in neurodegeneration. Brain 2017; 140: 266–278.

Goodkind M, Eickhoff SB, Oathes DJ, Jiang Y, Chang A, Jones-Hagata LB, et al. Identification of a common neurobiological substrate for mental Illness. JAMA Psychiatry 2015; 72: 305–315.

Green S, Higgins JP, Alderson P, Clarke M, Mulrow CD, Oxman AD. Introduction. In: Higgins JP, Green S, editor(s). Cochrane Handbook for Systematic Reviews of Interventions. Chichester, UK: John Wiley & Sons, Ltd; 2008. p. 1–9.

Guest WC, Silverman JM, Pokrishevsky E, O'Neill MA, Grad LI, Cashman NR. Generalization of the Prion Hypothesis to Other Neurodegenerative Diseases: An Imperfect Fit. J. Toxicol. Environ. Heal. Part A 2011; 74: 1433–1459.

de Haan W, Mott K, van Straaten ECW, Scheltens P, Stam CJ. Activity Dependent Degeneration Explains Hub Vulnerability in Alzheimer's Disease. PLoS Comput. Biol. 2012; 8

He Y, Chen ZJ, Evans AC. Small-world anatomical networks in the human brain revealed by cortical thickness from MRI. Cereb. Cortex 2007; 17: 2407–2419.

Iturria-Medina Y, Sotero RC, Toussaint PJ, Evans AC. Epidemic Spreading Model to Characterize Misfolded Proteins Propagation in Aging and Associated Neurodegenerative Disorders. PLoS Comput. Biol. 2014; 10

Janke AL, De Zubicaray G, Rose SE, Griffin M, Chalk JB, Galloway GJ. 4D deformation modeling of cortical disease progression in Alzheimer's dementia. Magn. Reson. Med. 2001; 46: 661–666.

Kapur S. Psychosis as a state of aberrant salience: A framework linking biology, phenomenology, and pharmacology in schizophrenia. Am. J. Psychiatry 2003; 160: 13–23.

Korth C. Aggregated proteins in schizophrenia and other chronic mental diseases. Prion 2012; 6: 134–141.

Laird AR, Lancaster JL, Fox PT. BrainMap: The Social Evolution of a Human Brain Mapping Database. Neuroinformatics 2005; 3: 065–078.

Lancaster JL, Tordesillas-Gutiérrez D, Martinez M, Salinas F, Evans A, Zilles K, et al. Bias between MNI and Talairach coordinates analyzed using the ICBM-152 brain template. Hum. Brain Mapp. 2007; 28: 1194–1205.

Lancaster JL, Woldorff MG, Parsons LM, Liotti M, Freitas CS, Rainey L, et al. Automated Talairach Atlas labels for functional brain mapping. Hum. Brain Mapp. 2000; 10: 120–131.

Laughlin SB, Sejnowski TJ. Communication in neuronal networks. Science (80-.). 2003; 301: 1870–1874.

Leliveld SR, Bader V, Hendriks P, Prikulis I, Sajnani G, Requena JR, et al. Insolubility of Disrupted-in-Schizophrenia 1 Disrupts Oligomer-Dependent Interactions with Nuclear Distribution Element 1 and Is Associated with Sporadic Mental Disease. J. Neurosci. 2008; 28: 3839–3845.

Liao XH, Xia MR, Xu T, Dai ZJ, Cao XY, Niu HJ, et al. Functional brain hubs and their test-retest reliability: A multiband resting-state functional MRI study. Neuroimage 2013; 83: 969–982.

Liberati A, Altman DG, Tetzlaff J, Mulrow C, Gotzsche PC, Ioannidis JPA, et al. The PRISMA statement for reporting systematic reviews and meta-analyses of studies that evaluate healthcare interventions: explanation and elaboration. BMJ 2009; 339: b2700–b2700.

Liddle EB, Price D, Palaniyappan L, Brookes MJ, Robson SE, Hall EL, et al. Abnormal salience signaling in schizophrenia: The role of integrative beta oscillations. Hum. Brain Mapp. 2016; 37: 1361–1374.

Loewenstein DA, Barker WW, Chang JY, Apicella A, Yoshii F, Kothari P, et al. Predominant left hemisphere metabolic dysfunction in dementia. Arch. Neurol. 1989; 46: 146–152.

Mancuso L, Costa T, Nani A, Manuello J, Liloia D, Gelmini G, et al. The homotopic connectivity of the functional brain: a meta-analytic approach. Sci. Rep. 2019; 9: 3346.

Mandelli ML, Vilaplana E, Brown JA, Hubbard HI, Binney RJ, Attygalle S, et al. Healthy brain connectivity predicts atrophy progression in non-fluent variant of primary progressive aphasia. Brain 2016; 139: 2778–2791.

Manoliu A, Riedl V, Zherdin A, Mühlau M, Schwerthöffer D, Scherr M, et al. Aberrant dependence of default mode/central executive network interactions on anterior insular salience network activity in schizophrenia. Schizophr. Bull. 2014; 40: 428–437.

Manuello J, Nani A, Premi E, Borroni B, Costa T, Tatu K, et al. The pathoconnectivity profile of Alzheimer's disease: A morphometric coalteration network analysis. Front. Neurol. 2018; 8: 1–15.

McTeague LM, Goodkind MS, Etkin A. Transdiagnostic impairment of cognitive control in mental illness. J. Psychiatr. Res. 2016; 83: 37–46.

Modinos G, Vercammen A, Mechelli A, Knegtering H, McGuire PK, Aleman A. Structural covariance in the hallucinating brain: A voxel-based morphometry study. J. Psychiatry Neurosci. 2009; 34: 465–469.

Moher D, Liberati A, Tetzlaff J, Altman DG. Preferred Reporting Items for Systematic Reviews and Meta-Analyses: The PRISMA Statement. J. Clin. Epidemiol. 2009; 62: 1006–1012.

Neckelmann G, Specht K, Lund A, Ersland L, Smievoll AI, Neckelmann D, et al. MR morphometry analysis of grey matter volume reduction in schizophrenia: Association with hallucinations. Int. J. Neurosci. 2006; 116: 9–23.

Palaniyappan L, Liddle PF. Does the salience network play a cardinal role in psychosis? An emerging hypothesis of insular dysfunction. J. Psychiatry Neurosci. 2012; 37: 17–27.

Palaniyappan L, White TP, Liddle PF. The Concept of Salience Network Dysfunction in Schizophrenia: From Neuroimaging Observations to Therapeutic Opportunities. Curr. Top. Med. Chem. 2013; 12: 2324–2338.

Patel RS, Bowman FD, Rilling JK. A Bayesian approach to determining connectivity of the

human brain. Hum. Brain Mapp. 2006; 27: 267–276.

Pievani M, de Haan W, Wu T, Seeley WW, Frisoni GB. Functional network disruption in the degenerative dementias. Lancet Neurol. 2011; 10: 829–843.

Plaze M, Bartrés-Faz D, Martinot JL, Januel D, Bellivier F, De Beaurepaire R, et al. Left superior temporal gyrus activation during sentence perception negatively correlates with auditory hallucination severity in schizophrenia patients. Schizophr. Res. 2006; 87: 109–115.

Raj A, Kuceyeski A, Weiner M. A Network Diffusion Model of Disease Progression in Dementia. Neuron 2012; 73: 1204–1215.

Rubinov M, Sporns O. Complex network measures of brain connectivity: Uses and interpretations. Neuroimage 2010; 52: 1059–1069.

Saxena S, Caroni P. Selective Neuronal Vulnerability in Neurodegenerative Diseases: From Stressor Thresholds to Degeneration. Neuron 2011; 71: 35–48.

Scarpazza C, Tognin S, Frisciata S, Sartori G, Mechelli A. False positive rates in Voxel-based Morphometry studies of the human brain: Should we be worried? Neurosci. Biobehav. Rev. 2015; 52: 49–55.

Seeley WW, Crawford RK, Zhou J, Miller BL, Greicius MD. Neurodegenerative Diseases Target Large-Scale Human Brain Networks. Neuron 2009; 62: 42–52.

Sepulcre J, Liu H, Talukdar T, Martincorena I, Thomas Yeo BT, Buckner RL. The organization of local and distant functional connectivity in the human brain. PLoS Comput. Biol. 2010; 6: 1–15.

Sheline YI, Barch DM, Price JL, Rundle MM, Vaishnavi SN, Snyder AZ, et al. The default mode network and self-referential processes in depression. Proc. Natl. Acad. Sci. 2009; 106: 1942–1947.

Sporns O, Zwi JD. The Small World of the Cerebral Cortex. Neuroinformatics 2004; 2: 145–

162.

Tatu K, Costa T, Nani A, Diano M, Quarta DG, Duca S, et al. How do morphological alterations caused by chronic pain distribute across the brain? A meta-analytic co-alteration study. NeuroImage Clin. 2018; 18: 15–30.

Thompson PM, Hayashi KM, Dutton RA, Chiang M-C, Leow AD, SowellL ER, et al. Tracking Alzheimer's Disease. Ann. N. Y. Acad. Sci. 2007; 1097: 183–214.

Thompson PM, Hayashi KM, de Zubicaray G, Janke AL, Rose SE, Semple J, et al. Dynamics of Gray Matter Loss in Alzheimer's Disease. J. Neurosci. 2003; 23: 994–1005.

Thompson PM, Mega MS, Woods RP, Zoumalan CI, Lindshield CJ, Blanton RE, et al. Cortical Change in Alzheimer's Disease Detected with a Disease-specific Population-based Brain Atlas. Cereb. Cortex 2001; 11: 1–16.

Trossbach S V., Bader V, Hecher L, Pum ME, Masoud ST, Prikulis I, et al. Misassembly of full-length Disrupted-in-Schizophrenia 1 protein is linked to altered dopamine homeostasis and behavioral deficits. Mol. Psychiatry 2016; 21: 1561–1572.

Turkeltaub PE, Eickhoff SB, Laird AR, Fox M, Wiener M, Fox P. Minimizing within-experiment and within-group effects in activation likelihood estimation meta-analyses. Hum. Brain Mapp. 2012; 33: 1–13.

Uddin LQ. Salience processing and insular cortical function and dysfunction. In: Nature Reviews Neuroscience. Nature Publishing Group; 2015. p. 55–61.

Vanasse TJ, Fox PM, Barron DS, Robertson M, Eickhoff SB, Lancaster JL, et al. BrainMap VBM: An environment for structural meta-analysis. Hum. Brain Mapp. 2018; 39: 3308–3325.

Watts DJ, Strogatz SH, Tseng Y-M. Collective dynamics of 'small-world' networks. Nature 1998; 153: 810–817.

Wheeler AL, Felsky D, Viviano JD, Stojanovski S, Ameis SH, Szatmari P, et al. BDNF-

Dependent Effects on Amygdala–Cortical Circuitry and Depression Risk in Children and Youth. Cereb. Cortex 2017; 28: 1760–1770.

Wheeler AL, Wessa M, Szeszko PR, Foussias G, Chakravarty MM, Lerch JP, et al. Further neuroimaging evidence for the deficit subtype of schizophrenia: A cortical connectomics analysis. JAMA Psychiatry 2015; 72: 446–455.

White TP, Joseph V, Francis ST, Liddle PF. Aberrant salience network (bilateral insula and anterior cingulate cortex) connectivity during information processing in schizophrenia. Schizophr. Res. 2010; 123: 105–115.

World Health Organisation. The ICD-10 classification of mental and behavioural disorders: clinical descriptions and diagnostic guidelines. World Heal. Organ. 1992

Zhou J, Gennatas ED, Kramer JH, Miller BL, Seeley WW. Predicting Regional Neurodegeneration from the Healthy Brain Functional Connectome. Neuron 2012; 73: 1216–1227.

Zhu S, Abounit S, Korth C, Zurzolo C. Transfer of disrupted-in-schizophrenia 1 aggregates between neuronal-like cells occurs in tunnelling nanotubes and is promoted by dopamine. Open Biol. 2017; 7

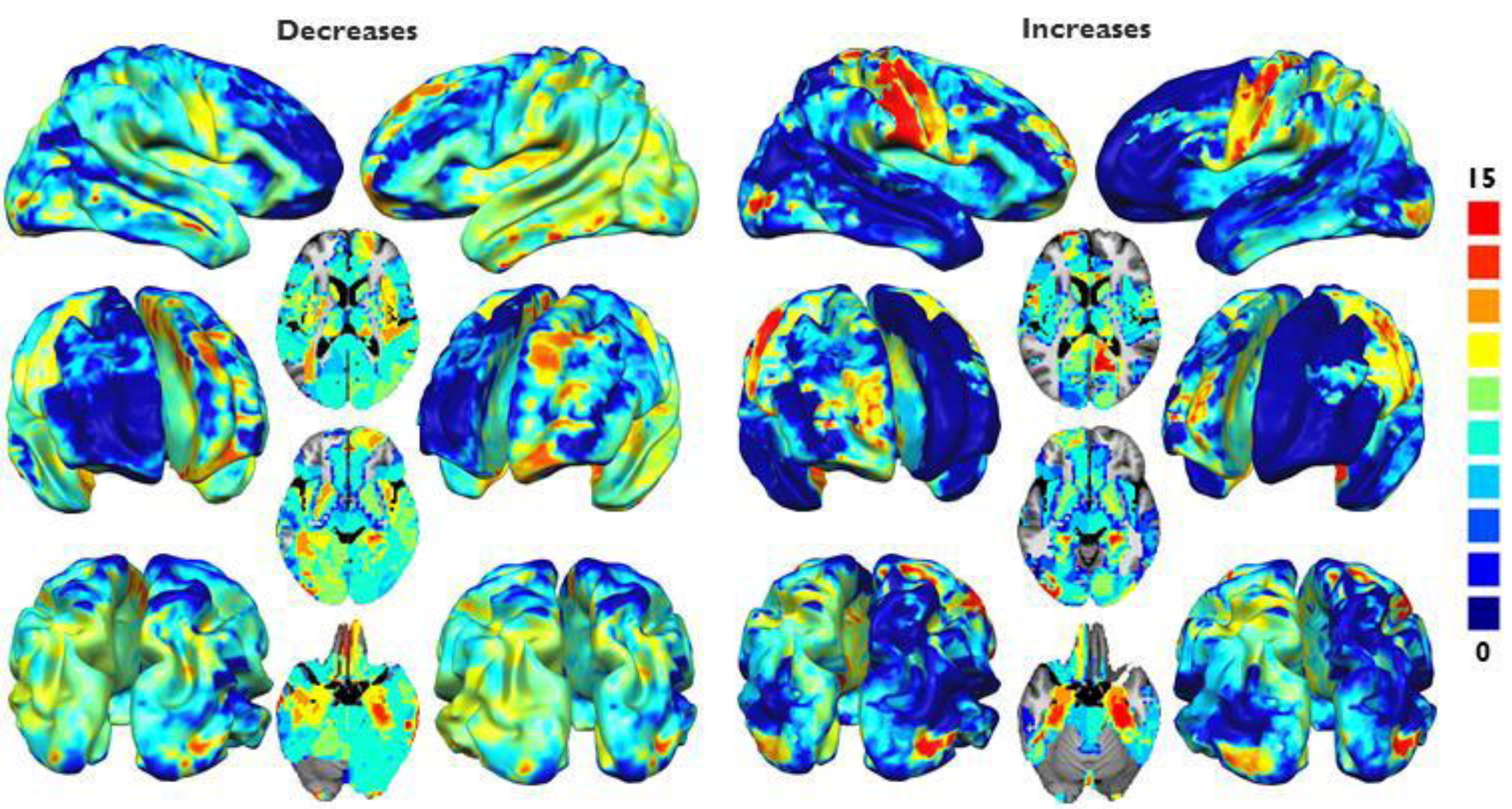
Decreases
Increases
15
0

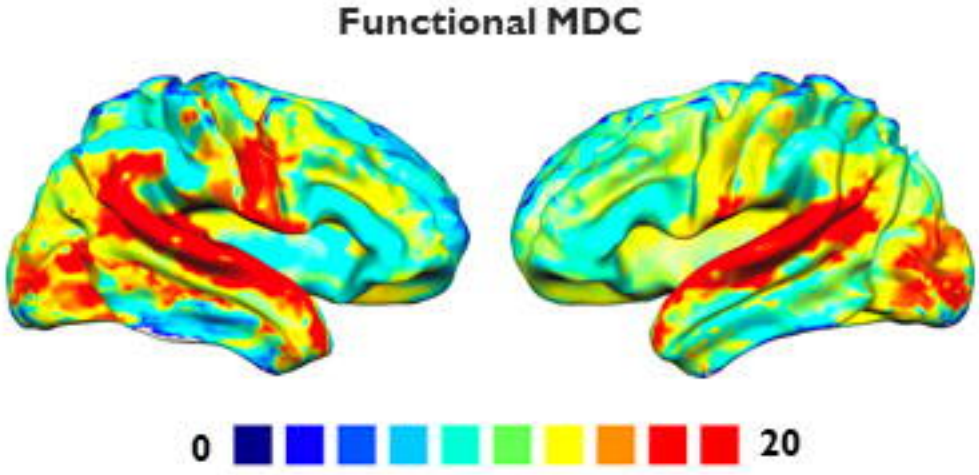
Functional MDC
0
20

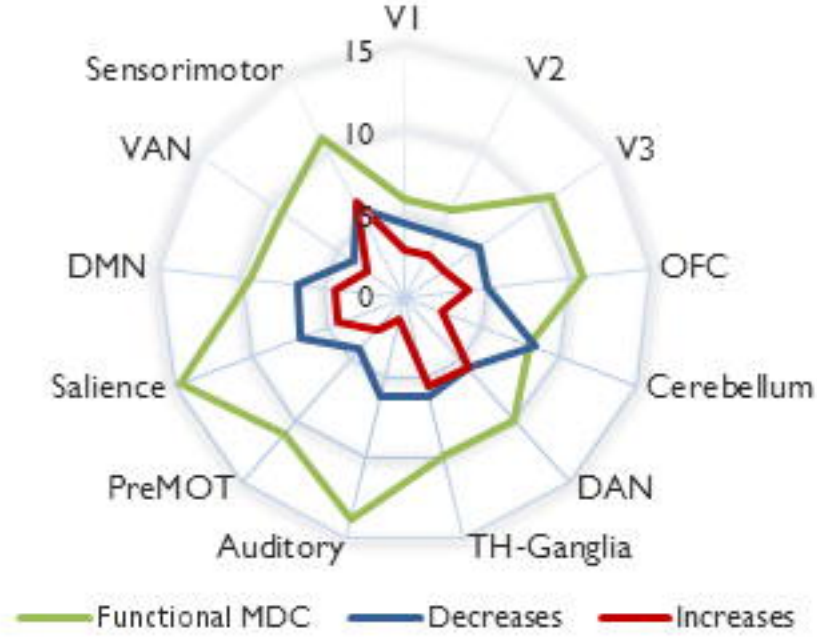
V1
V2
V3
OFC
Cerebellum
DAN
TH-Ganglia
Auditory
PreMOT
Salience
DMN
VAN
Sensorimotor
15
10
5
0
Functional MDC
Decreases
Increases

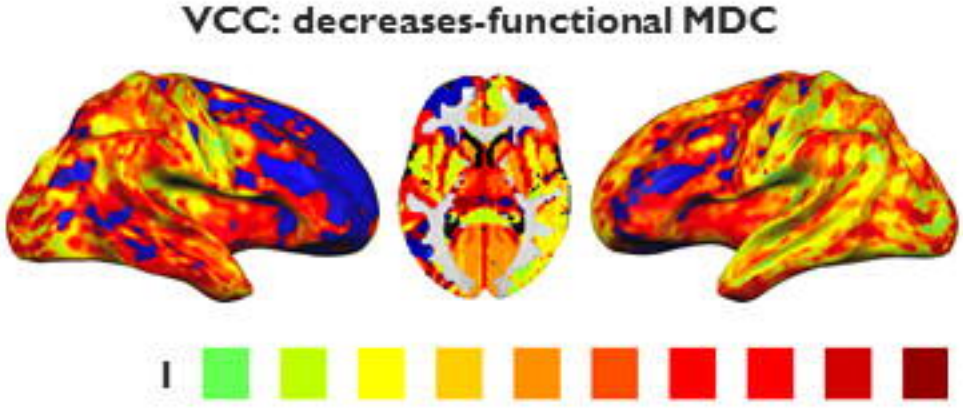
VCC: decreases-functional MDC
1
0

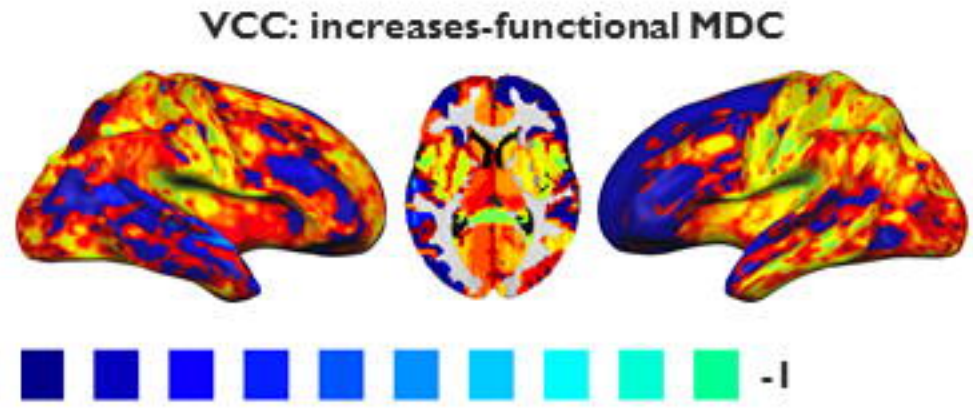
VCC: increases-functional MDC
0
-1

Leave one pathology out

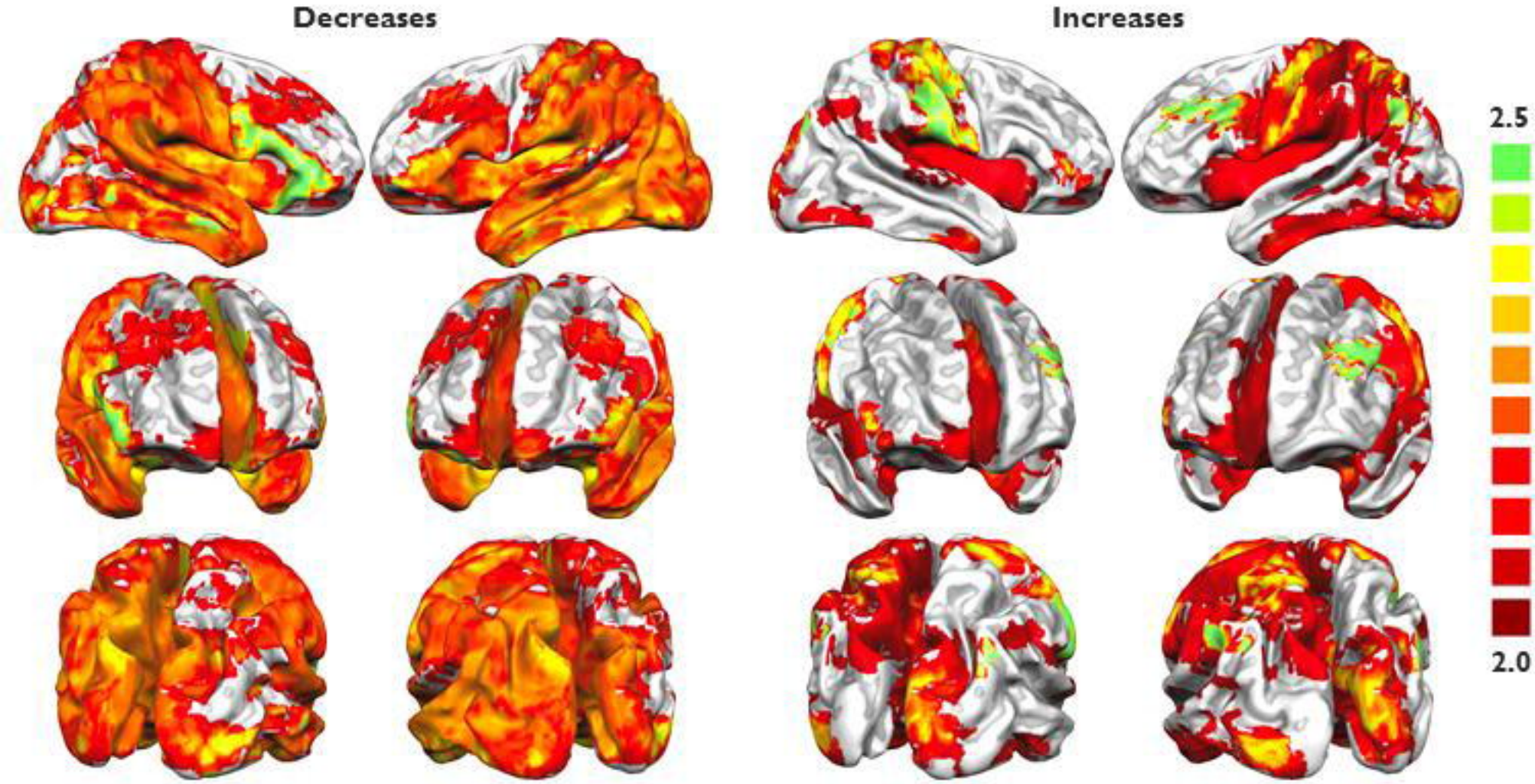

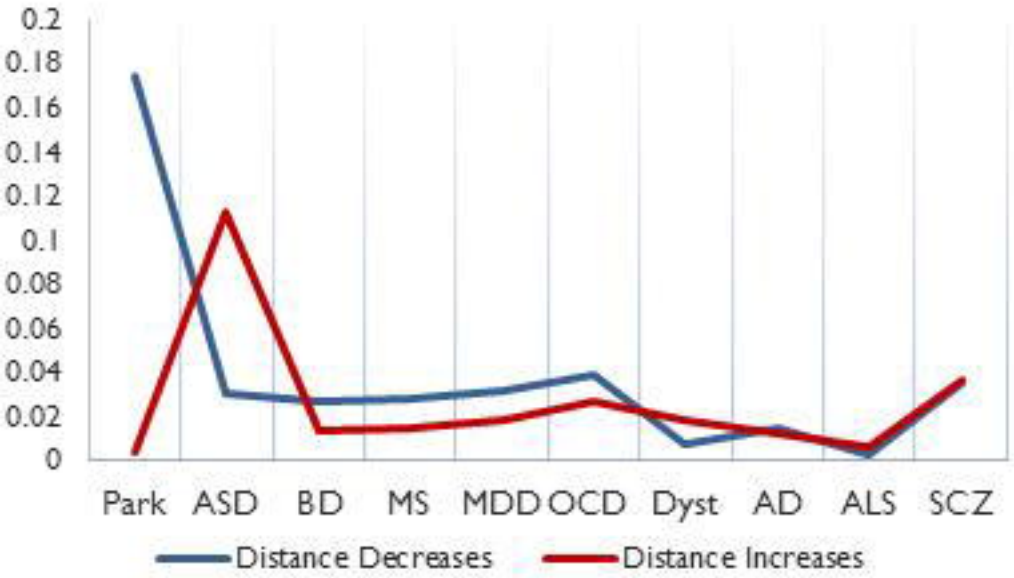

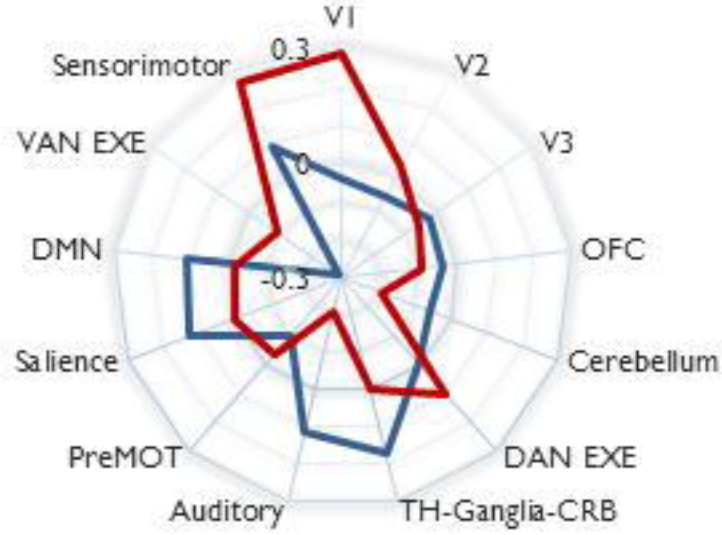

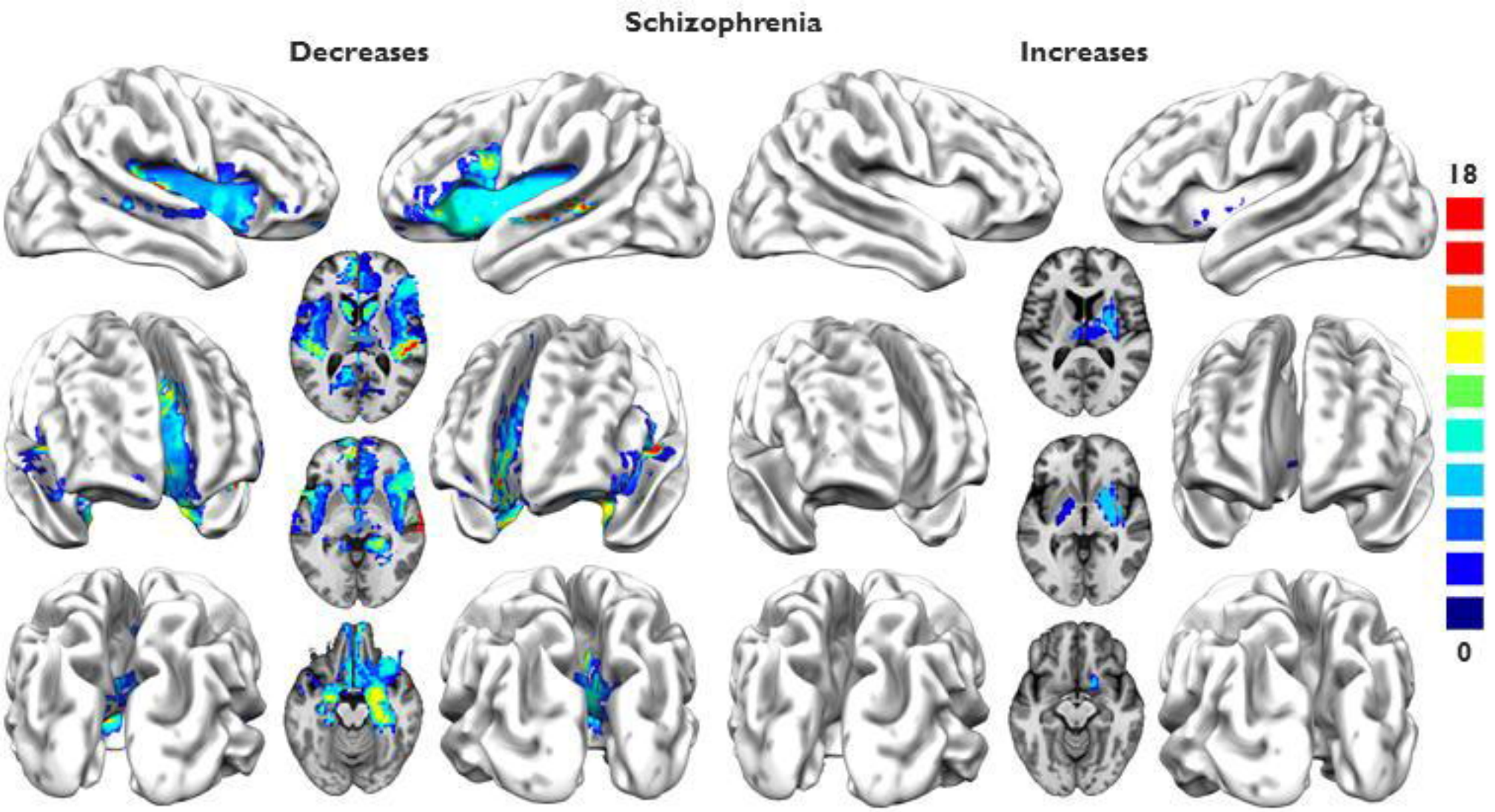
Schizophrenia
Decreases
Increases
18
0

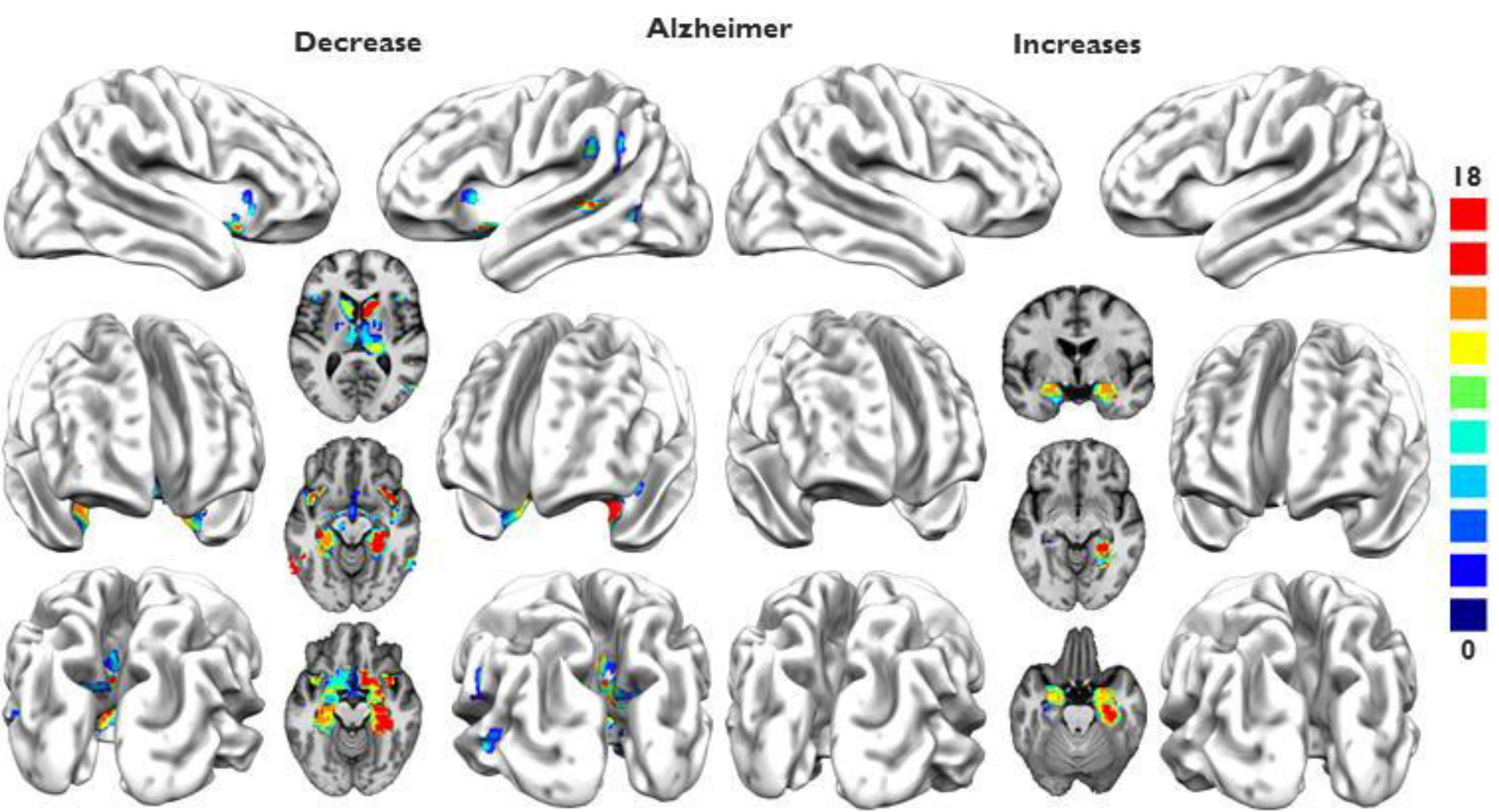
Decrease
Alzheimer
Increases
18
0